Polysialic Acid/Neural Cell Adhesion Molecule Modulates the Formation of Ductular Reactions in Liver Injury

PolySia-NCAM modulates the formation of ductular reactions in liver injury

Atsunori Tsuchiya[1,2], Wei-Yu Lu[1], Birgit Weinhold[3], Luke Boulter[1], Benjamin M Stutchfield[1], Michael J Williams[1], Rachel V Guest[1], Sarah E Minnis-Lyons[1], Alison C MacKinnon[1], David Schwarzer[3], Takafumi Ichida[4], Minoru Nomoto[2], Yutaka Aoyagi[2], Rita Gerardy-Schahn[3], Stuart J Forbes[1]

1. Medical Research Council Centre for Regenerative Medicine, SCRM Building The University of Edinburgh, Edinburgh bioQuarter, 5 Little France Drive, Edinburgh EH16 4UU, UK

2. Division of Gastroenterology and Hepatology, Graduate School of Medical and Dental Science, Niigata University, 1-757 Asahimachi-dori, Chuo-ku, Niigata, 951-8510, Japan

3. Institute for Cellular Chemistry, Hannover Medical School, Carl-Neuberg Str.1, D-30625 Hannover, Germany

4. Department of Hepatology and Gastroenterology, Juntendo Shizuoka Hospital, 1129 Izunokuni City, Shizuoka Prefecture, 410-2295, Japan

E-mail:

Atsunori Tsuchiya: atsunori@med.niigata-u.ac.jp

Wei-Yu Lu: w.y.lu@ed.ac.uk

Birgit Weinhold: Weinhold.birgit@mh-hannover.de

Luke Boulter: lboulter@staffmail.ed.ac.uk

Benjamin M Stutchfield: benstutch@gmail.com

Michael J Williams: mike.williams@doctors.org.uk

Rachel V Guest: rvguest@doctors.org.uk

Sarah E Minnis-Lyons: saraheminnis@aol.com

Alison C MacKinnon: a.mackinnon@ed.ac.uk

David Schwarzer: david.schwarzer@abbott.com

Takafumi Ichida: takafumi@air.ocn.ne.jp

Minoru Nomoto: mnomoto@med.niigata-u.ac.jp

Yutaka Aoyagi: aoy@med.niigata-u.ac.jp

Rita Gerardy-Schahn: Gerardy-schahn.rita@mh-hannover.de

Stuart J Forbes: stuart.forbes@ed.ac.uk

Key Words: NCAM, polysialic acid, hepatic progenitor cell, ductular reaction, niche

Corresponding Author: Stuart J. Forbes

Address: SCRM Building The University of Edinburgh, Edinburgh bioQuarter, 5 Little France Drive, Edinburgh EH16 4UU, UK

Tel: +44 131 651 9515

Fax: +44 131 651 9501

E-mail address: stuart.forbes@ed.ac.uk

Abbreviations;

NCAM, neural cell adhesion molecule; polySia, polysialic acid; HPC, hepatic progenitor cell; NHNPC, non-hepatic progenitor cell neural cell adhesion molecule positive cell; endoN, endosialidase; CDE, choline-deficient ethionine-supplemented; DDC, 3,5-diethoxycarbonyl-1,4-dihydrocollidine; DR, ductular reaction; OSM, oncostatin M; HCC, hepatocellular carcinoma; panCK, pancytokeratin; GGT, γ-glutamyl transpeptidase; GFAP, glial fibrillary acidic protein; RT, room temperature; EPCAM, epithelial cell adhesion molecule; TAT, tyrosine aminotransferase; CPS1, carbamoyl phosphate synthetase 1; To, tryptophan-2, 3-dioxygenase; G6p, glucose 6 phosphatase; Prom-1, prominin-1; Col-1, collagen 1; TB, total bilirubin; ALP, alkaline phosphatase; ALB, albumin; AST, aspartate aminotransferase; ALT, alanine aminotransferase; cyp, cytochrome P450;

Number of Figures, Videos and Tables; 8 figures, 2 supplemental tables, 9 supplemental figures and 2 supplemental videos.

Disclosures; The authors declare no conflict of interest.

Acknowledgments; The authors thank Professor Frederic A. Troy II (University of California School of Medicine) and Professor Ken Kitajima (Nagoya University) for giving us critical comments on our study. The TROMA-III antibody developed by Rolf Kemler was obtained from the Developmental Studies Hybridoma Bank developed under the auspices of the NICHD and maintained by The University of Iowa, Department of Biology, Iowa City, IA 52242.

Financial Support; This work was supported by Daiichi-Sankyo Foundation of Life Science and The Medical Research Council, UK. The German partners (RGS, DS and BW) acknowledge financial support via the cluster of excellence REBIRTH.

ABSTRACT

In severe liver injury ductular reactions (DRs) containing bipotential hepatic progenitor cells (HPCs) branch from the portal tract. Neural cell adhesion molecule (NCAM) marks bile ducts and DRs but not mature hepatocytes. NCAM mediates interactions between cells and surrounding matrix, however its role in liver development and regeneration is undefined. Polysialic acid (polySia), a unique posttranslational modifier of NCAM is produced by the enzymes ST8SiaII and ST8SiaIV and weakens NCAM interactions. The role of the polySia with NCAM synthesising enzymes St8SiaII and St8SiaIV were examined in HPCs *in vivo* using the CDE and DDC diet models of liver injury and regeneration, *in vitro* using models of proliferation, differentiation and migration and by use of mouse models with gene defects in the polysialyltransferases (*St8sia* $2^{+/-}4^{+/-}$, and *St8sia2*$^{-/-}4^{-/-}$). We show that during liver development, polySia is required for the correct formation of bile ducts as gene defects in both the polysialyltransferases (*St8sia2*$^{+/-}4^{+/-}$ and *St8sia2*$^{-/-}4^{-/-}$ mice) caused abnormal bile duct development. In normal liver there is minimal polySia production and few ductular NCAM+ cells. Following injury NCAM+ cells expand and polySia is produced by DRs/HPCs through ST8SiaIV. PolySia weakens cell-cell and cell-matrix interactions facilitating HGF induced migration. Differentiation of HPC to hepatocytes *in vitro* results in both transcriptional down-regulation of polySia and cleavage of polySia-NCAM. Cleavage of polySia by endosialidase (endoN) during liver regeneration reduces migration of DRs into parenchyma. ***Conclusion:*** We conclude that polySia modification of NCAM+ ductules weakens cell-cell and cell-matrix interactions allowing DRs/HPCs to migrate for normal development and regeneration. Modulation of polySia levels may provide a therapeutic option in liver regeneration.

INTRODUCTION

The normal liver regenerates efficiently through hepatocyte division. However, in chronic or severe liver injury a second regenerative compartment is activated termed the ductular reaction (DR)[1]. In severe liver injury DRs spread from the periportal area into the hepatic parenchyma. Hepatic progenitor cells (HPCs) are thought to reside in the Canal of Hering and expand after severe or chronic liver damage and regenerate hepatocytes and cholangiocytes. Clonogenic bipotential HPCs can be isolated from mice with DRs[2] and recent lineage tracing in mouse models of liver injury demonstrated that HPCs within the DR can regenerate parenchyma[3]. A stereotypical niche of cellular components (myofibroblasts and macrophages) which direct HPC mediated liver regeneration via Notch and Wnt signalling[4] surrounds the DRs[5]. Laminin matrix surrounds the DRs and may influence HPC behaviour. There is little information regarding the mechanisms controlling migration of HPCs/DRs or the detachment of cells from the cellular or acellular components of the niche[5].

In this report we have examined the functional role of the DR/HPC marker NCAM (neural cell adhesion molecule) and its typical posttranslational modification polysialic acid (polySia) in the DR/HPC niche. NCAM is a prototypic member of the immunoglobulin (Ig) family of adhesion molecules[6]. NCAM has three major isoforms; NCAM-120 (120kDa), -140 (140kDa) and -180 (180kDa). NCAM mediates cell-cell adhesion by multiple modes including homophilic and heterophilic interactions and cell-matrix contact[7]. These interactions are modified by the posttranslational modification of NCAM with polySia. Two Golgi-resident polysialyltransferases (polySTs) ST8SiaII and ST8SiaIV exist and transfer polySia onto complex N-glycans located in the fifth Ig-like domain of NCAM[8]. The enzymes ST8SiaII and ST8SiaIV are independently able to transfer polySia onto NCAM[9].

Due to the size of the polySia chains and their high water binding capacity polySia on NCAM (polySia-NCAM) changes NCAM functions from adhesive to anti-adhesive[10]. Accordingly, polySia-NCAM has been implicated in dynamic processes such as cell migration and plasticity in the nervous system[11]. The crucial role of polySia in ontogeny is highlighted by the lethal phenotype of

mice lacking two polySTs[12]. Mice with only partially depleted polySia synthetic capacity exhibit distinct but milder phenotypes[13]. The only known polySia degrading enzyme is endosialidase (endoN), a phage born enzyme[14]. Due to its stability and selectivity, endoN has been used in numerous animal models without producing adverse effects and we have therefore used endoN here to cleave polySia[15].

The liver has been described as an organ with low NCAM and polySia expression[12]. However, NCAM can be detected on specific cells in liver injury. Knittel et al. (1996) and Nakatani et al. (1996 and 2006) reported NCAM+ hepatic stellate cells and portal fibroblast in rat and human liver[16-18]. Fabris et al. (2000) reported that human reactive ductules with atypical morphology coexpressed NCAM[19, 20]. Zhou et al. (2007) provided evidence that NCAM+ cells in the DRs represent bipotent HPCs in human[21]. This study and our previous study[22] showed NCAM expression in bile ducts and a wide range of human DRs. Importantly those DRs immediately adjacent to mature hepatocytes were NCAM negative[21]. The biological functions of NCAM have not been previously reported in liver. Given that cell proliferation and migration from the niche is seen in liver regeneration, we hypothesized that the antagonistic functions of NCAM and polySia-NCAM in the regulation of cell adhesion and cell migration (proven for the nervous tissue) may play a significant role during liver development and regeneration.

Here we show for the first time the expression of polySia in the liver. PolySia was found to increase markedly after liver damage and facilitated the migration of the DRs/HPCs away from the periportal niche during liver regeneration. Furthermore polySia and its carrier NCAM were reduced during the differentiation of HPCs to mature hepatocytes.

MATERIALS AND METHODS

Mice

Animals were housed in a specific pathogen free environment and kept under standard conditions with a 12 hour day/night cycle and access to food and water *ad libitum*. All animal experiments had local ethical approval and were conducted according to UK Home Office Legislation. Male mice were fed either CDE (Choline Deficient Diet with 0.15% Ethionine diet; Sigma-Aldrich, St Louis, MO) or DDC diet (3,5-diethoxycarbonyl-1,4-dihydrocollidine; 0.1% Purina 5015 mouse chow) for 11 days to C57BL/6 mice (n=6, 7 weeks old) and S129P2 mice (n=6, Halran Laboratories, Inc. Indianapolis, IN, 10 weeks old) respectively for immunohistochemistry and real-time PCR. To analyse the effect of endoN during liver development, 6 wild type mice, 7 double heterozygous *St8sia2*$^{+/-}$*4*$^{+/-}$ mice and 12 double knock out *St8sia2*$^{-/-}$*4*$^{-/-}$ mice (provided by Professor Rita Gerardy-Schahn, Hannover University) were analysed. All wild type and *St8sia* mutant mice were sacrificed at day P8.5-P9.5. To analyse the effect of endoN during liver regeneration, S129P2 mice (more than 10 weeks old) were fed DDC diet for 16 days. Induction of polySia was significantly higher in DDC diet mouse liver compared to CDE diet mouse liver (Figure 1C and D), thus we employed the DDC diet mice in this experiment. To determine an effective dose of endoN that would work *in vivo*, we injected 3.14-19.69 μg of endoN/g of mouse in a single intraperitoneal injection on day 15 of a 16 day DDC injury protocol. While all of the control injected mice were positive for polySia in western blots of whole liver tissue lysates, polySia could not be detected in the endoN injected mouse liver tissue lysates (Supplemental figure 8B). As side effects were not seen with any endoN dose, 5μg/g/injection of endoN was used in the subsequent experiment and was injected 4 times (days 8, 10, 12 and 14) intraperitoneally during the 16 day DDC experiment (Supplemental figure 8A). Mice were divided into two groups, one group received endoN (n=10) and control mice received vehicle (n=9). Histological analysis, liver weight/body weight (LW/BW) ratio, serum blood tests and real-time PCR were performed for analysis. Serum was analysed using commercial kits for: Alanine aminotranspherase (ALT; Alpha Laboratories Ltd, Eastleigh, UK), Albumin (Olympus Diagnostics Ltd, Southend-on Sea, UK), Aspartate

Aminotransferase (AST) and Alkaline Phosphatase (ALP) (both Randox Laboratories, London, UK) according to manufacturer's instructions.

Further description of the materials and methods used are provided in the supplemental file.

RESULTS

NCAM+ DRs expand from the periportal area after liver injury

We studied immunohistochemistry for NCAM from mouse models of hepatocellular injury and regeneration (CDE diet) and from biliary injury and regeneration (DDC diet). In normal livers, a few bile duct cells and their surrounding cells were positive for NCAM, however after liver damage NCAM+ DRs and closely associated NCAM+ niche cells began to expand from the portal area and spread into the parenchyma in both hepatocellular and biliary injury (Figure 1A and B). These results suggested that NCAM+ cells are at least two populations, the epithelial cells of the DR and their surrounding niche cells following liver damage.

ST8SiaIV is the main polysialyltransferase expressed in damaged mouse livers

Two enzymes, the polySTs ST8SiaII and IV are independently able to transfer polySia onto NCAM. The levels of polyST transcripts have been demonstrated to tightly correlate with the level of polySia expression[23]. To identify the polySTs responsible for NCAM polysialylation in the liver, the gene expression levels were determined in parallel to *Ncam* expression in the CDE and DDC damaged livers. Both diets (CDE shown in Figure 1C and DDC in Figure 1D) led to a significant increase in the expression of *Ncam* and *St8sia4*, while the expression of *St8sia2* remained at the level of control tissue. Since the product formation by polySTs has been described to be tightly linked to the mRNA expression level this data provides strong evidence that polySia production in damaged livers results from ST8SiaIV activity[23].

Ductular cells and myofibroblasts surrounding the DRs are NCAM+ and polySia is predominantly expressed at the lateral cell surface of bile ducts and DRs

To precisely define the NCAM+ cells associated with the DRs in 11 day DDC damaged livers, double fluorescence immunohistochemistry was performed using NCAM together with markers for bile ducts and DRs (panCK and sox9; panCK can stain bile ducts and DRs/HPCs in the same manner with

cytokeratin19 (CK19) as Supplemental figure 1A and B. Both anti-panCK and anti-CK19 antibodies were used in this study), hepatic stellate cells (desmin and GFAP), myofibroblasts (α-SMA and desmin) and hematopoietic cells (CD45). Double immunofluorescence between NCAM, and panCK (Figure 2A and Supplemental figure 2A) and sox9 (Figure 2B and Supplemental figure 2B) revealed that bile duct and DRs (epithelial cells) frequently expressed NCAM, together with surrounding (non-epithelial) cells. α-SMA+/NCAM+ cells and desmin+/NCAM+ cells were identified to associate with the DRs, however, α-SMA-/NCAM+ and desmin-/NCAM+ cells were also detected in this area (Figure 2C and Supplemental figure 2C). We could not detect GFAP+/NCAM+ cells (Supplemental figure 2D) or CD45+/NCAM+ cells (Supplemental figure 2E). These results revealed that there are NCAM+ myofibroblasts associated with the DRs. When the relationship between NCAM+ cells and laminin (Supplemental figure 2F) was analysed in the DRs, it was found that almost all NCAM+ cells made contact with laminin. PolySia was predominantly located at the lateral cell surface of bile ducts and DRs (Figure 2D). NCAM and polySia also could be detected in the same manner in the long term (8 weeks) DDC damaged livers (Supplemental figure 2G and H) suggesting that polySia-NCAM system is perpetuated during liver damage. Furthermore to analyse polySia-NCAM in human chronic liver diseases, we immunostained for CK19, NCAM and polySia using serial sections of cirrhotic liver tissues caused by hepatitis C virus (HCV), alcohol and primary biliary cirrhosis (PBC). All of these human diseases expressed NCAM and polySia in DRs suggesting that polySia-NCAM is present in human chronic liver diseases (Figure 3E).

PolySia weakens cell-matrix interactions, prevents cell aggregation and promotes HGF induced migration of HPCs in HPC culture models

To analyse the role of polySia we stained three HPC lines, previous characterized HPC line BMOL [24] and our two established cell lines (HPC line 2 and 3), for NCAM and polySia. All of the HPC lines expressed NCAM and polySia (Figure 3A and Supplemental figure 3A and B). BMOLs had 6 times the expression level of polySia compared to other two HPC lines (Supplemental figure 3C) and showed

typical gene changes seen during a differentiation protocol induced by Wnt3A or OSM with a decrease in *Ck19* and an increase in the hepatocyte markers *Alb* (Supplemental figure 4A and C). HGF induced relatively weak differentiation (Supplemental figure 4B), but induced HPC expansion and migration *in vitro* (Figure 3C and E). Therefore the BMOL cells are an ideal HPC line for further analysis of polySia and NCAM. Flow cytometric analysis revealed that BMOLs are almost all positive for NCAM but have varying levels of polySia positivity (Figure 3A). To investigate the polySia-NCAM relationship further western blot analysis for NCAM was performed using wild type P1.5 neonatal mouse brain (known to contain abundant polySia-NCAM as positive control), P1.5 NCAM knock out neonatal mouse brain (negative control) and BMOLs with or without endoN. Without endoN a diffuse signal around 200kDa was seen which showed polySia with NCAM in wild type P1.5 neonatal mouse brain lane and BMOLs lane. After treatment with polySia specific endoN, bands were concentrated at 180kDa and 140kDa in the wild type P1.5 neonatal mouse brain lane and at 140kDa in BMOLs lane respectively. In NCAM knock out mouse lanes no band could be detected (Figure 3A). To confirm the relationship between NCAM and polySia further co-immunoprecipitation was performed. Following immunoprecipitation for NCAM, immunoprecipitates were blotted for NCAM and polySia. This showed the polySia with NCAM diffuse signal (around 200kDa) in both groups. After endoN digestion, western blot for NCAM showed that this signal was concentrated at 140kDa (Supplemental figure 5). All of these results indicate that NCAM-140 is the main carrier of polySia in the BMOL HPC cell line (Figure 3A). As seen in whole mouse liver, *St8sia4* was also the main polyST in BMOL by RT-PCR (Supplemental figure 6A). We examined the laminin-BMOL cell-matrix interaction by seeding BMOL cells on laminin-coated plates for 30 minutes. Pre-treatment with endoN significantly increased cell adhesion compared to control (Figure 3B) suggesting that polySia weakens the cell-matrix interaction in the HPC niche.

We examined whether polySia impacts upon HPC expansion, aggregation, and migration with or without endoN. We assessed BMOL expansion with or without HGF having confirmed that cell expansion induced by HGF for 3 days culture did not affect NCAM expression levels in the BMOLs (Supplemental figure 6B). In both groups, cleavage of polySia by endoN did not affect cell expansion

(Figure 3C). In contrast aggregation assays revealed that the presence of endoN decreased (>10%) significantly the ratio of single cells/total cells (55.1±3.1 vs 44.9±3.3%) (Figure 3D), suggesting that polySia inhibits formation of stable cell-cell aggregation. Migration assays with a strong migratory stimulation factor HGF showed that endoN significantly decreased cell migration (6.53±0.28e^5 pixel vs 5.93±0.26e^5 pixel), however in the absence of migratory stimulation the difference was not obvious (Figure 3E). Taken together these results sugget that polySia inhibits cell-cell and cell-matrix interactions and promotes HPC migration in response to HGF.

PolySia-NCAM is cleaved during differentiation of HPCs to hepatocytes by OSM

While DRs/HPCs themselves express polySia and NCAM, hepatocytes were negative for both factors suggesting that during differentiation, polySia-NCAM disappears from the cell surface of HPCs. We therefore checked the fate of polySia during differentiation to hepatocyte-like cells through the addition of Wnt3A, HGF and OSM to BMOLs[25] by flow cytometry and found that the frequency of polySia+ cells decreased significantly compared to untreated cells (Figure 4A and B) 2 and 4 days after the addition of Wnt3A, HGF and OSM. Four days following the addition of OSM the frequency of polySia+ cells decreased markedly. We further checked the effect of Wnt3A, HGF and OSM upon polySia transcription by looking for changes in *Ncam* and *St8sia4* mRNA at day1. Wnt3A and HGF decreased *St8sia4* mRNA at day1 and the frequency of polySia+ cells by flow cytometry at day2 suggesting that Wnt3A and HGF decreased polySia at the transcriptional level. However OSM increased *Ncam* and *St8sia4* gene expression at day1 and decreased the frequency of polySia+ cells by flow cytometry significantly at day2 indicating that during OSM induced differentiation the reduction in polySia+ cells was not mediated at the transcriptional level (Figure 4C). Because the antibody used in flow cytometry recognized polySia and not NCAM, to resolve the mechanism of polySia disappearance western blot for NCAM using 24h BMOL cultures separated into cell lysate and supernatant was performed. This revealed that the protein level of NCAM after endoN treatment in BMOL cell lysate decreased after addition of OSM (Figure 4D) and the protein level of NCAM after endoN treatment in the BMOL

supernatant increased after the addition of OSM (Figure 4E). These results support the idea that NCAM was cleaved and released to the supernatant during differentiation.

Hepatic myofibroblasts contain NCAM+ cells with low polySia expression *in vitro*

We previously identified NCAM+ DR-associated myofibroblasts and we therefore established two non-epithelial NCAM+ cell lines from CDE damaged livers; (non-hepatic progenitor cell neural cell adhesion molecule positive cells) NHNPC1 and NHNPC2. Both sub-fractions contained NCAM+ and α-SMA+ cells (Figure 5A). Both fibroblastic cell lines contained hepatic myofibroblasts that expressed mRNA for myofibroblasts (*α-sma*, *Fibulin-2*, *Collagen-1* and *Desmin)* but were negative for the inactivated hepatic stellate cell marker *Gfap* (Figure 5B). Importantly flow cytometric analysis revealed that while the polySia expression levels in HPC cell lines were high (Supplemental figure 3C), polySia expression levels in NHNPCs were low (Figure 5C).

EndoN digestion of polySia reduces HPC migration in co-cultures with myofibroblasts

We analysed BMOL migration with myofibroblasts to model the cellular interactions in the damaged regenerating liver. We therefore modeled an “artificial niche” by culturing BMOLs upon a NHNPC1 cell layer with or without endoN (Figure 5D). Time lapse photography revealed that red stained BMOLs readily migrate over the myofibroblasts, however in the presence of endoN the mobility of the BMOLs was significantly decreased (Supplemental video 1; control and 2; with endoN). The average distance of migration dropped by >30% (from 97.4±47.0μm to 62.1±31.6μm) in endoN containing cultures (Figure 5E) indicating that polySia weakens the HPC cell-cell interaction and thus aids migration of the DRs/HPCs.

PolySia is required for the correct formation of bile ducts

We isolated and expanded fetal HPCs from C57BL/6 mice[25] and confirmed that they expressed NCAM (Figure 6A) and polySia (Figure 6B). To understand further the role of polySia in liver development we

analysed the neonatal (8.5-9.5 days after birth) livers of wild type, heterozygous *St8sia2*$^{+/-}$*4*$^{+/-}$ and double knock out *St8sia2*$^{-/-}$*4*$^{-/-}$ mice. Since most of the double KO mice die within 20 days after birth, we analysed the livers from 8.5-9.5 day old neonatal mice. H&E staining of these livers revealed an obvious difference between wild type livers and *St8sia2*$^{+/-}$*4*$^{+/-}$ or *St8sia2*$^{-/-}$*4*$^{-/-}$ mice which lacked proper bile duct structures (Figure 6C). To confirm this we performed immunohistochemistry for panCK (Figure 6C) and quantified the tube forming bile ducts (bile ducts with typical morphology)/portal area in all groups. The frequency of tube forming bile ducts/portal area in *St8sia2*$^{+/-}$*4*$^{+/-}$ and *St8sia2*$^{-/-}$*4*$^{-/-}$ mice group was decreased significantly compared to the wild type group (Figure 6D, Supplemental figure 7). We performed real-time PCR using bile duct and HPC markers (*Ck19* and *Ggt* and *Sox9*, *Prominin-1*, *Ncam* and *Epcam*) and hepatocyte markers (*Alb*, *Tat*, *Cps1*, *To*, *G6p*, *Cyp1a2* and *Cyp2a12*) from each group. There were no significant differences between wild type and *St8sia2*$^{+/-}$*4*$^{+/-}$ mice except the increase of the mRNA levels of *Ck19*, which is expressed in bile ducts and DRs, in *St8sia2*$^{+/-}$*4*$^{+/-}$ mice. In contrast, there were marked differences between wild type and *St8sia2*$^{-/-}$*4*$^{-/-}$ mice with up-regulation of many biliary and HPC marker genes in *St8sia2*$^{-/-}$*4*$^{-/-}$ mice (Figure 6E).

PolySia is required for the migration of DRs into the liver parenchyma in the DDC diet liver damage model

To confirm the role of polySia during liver regeneration *in vivo,* we injected mice intraperitoneally with endoN during the DDC induced liver injury protocol (Supplemental figure 8A).

Most obvious difference was the formation of DRs. In endoN injected group most of the DRs stayed in the portal area, in contrast in control group DRs migrating into the liver parenchymal area were more obvious (Figure 7A and B, and Supplemental figure 9). Furthermore, in the endoN injection group the liver weight/body weight (LW/BW) ratio was lower and serum levels of alanine aminotransferase (ALT) were higher compared to the control injection group (Figure 7C and D). Finally, we cecked the mRNA expression of bile duct and HPC markers (*Ck19* and *Ggt and Sox9*, *Prominin-1*, *Ncam* and *Epcam*), hepatocyte markers (*Alb*, *Tat*, *Cps1*, *To*, *G6p*, *Cyp1a2* and *Cyp2a12*) and fibrosis related markers

(*α-sma*, *Desmin* and *Collagen-1*). The mRNA of *Ck19*, *Alb*, *Tat*, *Cps1* and *Collagen-1* were increased in the endoN injection group compared to controls (Figure 7E). Overall, these results suggest that the endoN injection cleaves the hepatic polySia, resulting in less ductular migration and an increase susceptibility to hepatocellular injury during DDC diet liver damage.

DISCUSSION

The regeneration of hepatocytes and biliary epithelia by HPCs has been demonstrated using lineage tracing techniques[26]. However, the trigger for the formation of the DRs and detachment of HPCs from the niche into hepatocytes or bile ducts is not well understood. PolySia, through its action in weakening cell-cell and cell-matrix interactions contributes to this important step during liver regeneration.

In the brain, the roles of NCAM and polySia have been extensively analysed and the physicochemical properties of the large and highly hydrated polySia have been implicated in the modulation of cell-cell contact. The presence of polySia enhances migration of neural progenitor cells and the growth and targeting of axons[11]. Our studies have shown that in the normal liver NCAM expressing cells are very limited in number and are confined to bile duct cells and fibroblasts near the portal tract. However, after liver damage, NCAM+ cells and polySia production begin to increase in the area of the DR/HPC niche. Both ductular and non-ductular cells surrounding the DR express NCAM. HPCs have high levels of polySia and the main HPC polyST was ST8SiaIV, whilst myofibroblasts have low levels of polySia expression. In damaged livers the main polyST was ST8SiaIV, which is consistent with a predominant HPC source. From these results, we conclude that HPCs produce polySia mainly through ST8SiaIV, and that this is the main mechanism by which polySia is produced in the DR/HPC niche of damaged livers. PolySia is predominantly expressed at the lateral cell surface of the DRs and bile ducts. *In vitro* studies using a HPC cell line revealed that polySia weakens cell-matrix interaction and cell-cell aggregation of HPCs and increases HGF induced HPC migration. While the NCAM expression in HPCs is described, the fate of NCAM is not known as their progeny the hepatocytes do not express NCAM. Here we show that NCAM is cleaved during OSM induced differentiation of HPCs to hepatocytes and suggest it likely that NCAM and polySia-NCAM is cleaved from HPCs as soluble NCAM during the differentiation of HPCs into hepatocytes in damaged livers.

In mice lacking polySia expression (*St8sia2*$^{-/-}$*4*$^{-/-}$ double knock-out mice), severe phenotypic alterations

have been described in the brain suggesting a lack of neural plasticity due to a precocious presentation of polySia free NCAM forms[12]. In the liver of neonatal double knock-out mice, tube forming bile duct formation was inhibited and many HPC markers and bile duct markers were up-regulated, suggesting that polySia is required for correct liver as well as brain development.

The role of polySia in liver regeneration was analysed in the DDC induced liver damage model by repeated endoN injection. DRs/HPCs in the endoN injected polySia cleaved mice migrated less compared to controls suggested that polySia promotes effective migration of DRs/HPCs during liver regeneration. This endoN injected mice were increased susceptibility to liver damage with increasing the serum levels of ALT compared to controls. Adverse effects of endoN have not been reported to date, however from these experiments we found that endoN may exacerbate hepatocellular injury. We would therefore not advocate the clinical use of this compound in the setting of liver injury.

Data showing the presence of polySia-NCAM on short-term and long-term mouse DRs and on human DRs in chronic liver diseases suggest polySia-NCAM system is perpetuated during liver damage, is not species-specific and has potential relevance in human liver disease. Recently other function of polySia is reported including a role as a reservoir for neurotrophic factors and neurotransmitters[27]. It will be interesting in future studies to determine whether polySia has such roles in liver development and regeneration.

NCAM is by far the best characterized and major polySia carrier[28], however recently other polySia binding protein such as SynCAM1[29], neuropilin-2[30] and Myristoylated Alanine-rich C kinase Substrate (MARCKS)[31] have been reported. Of these binding proteins polysialylation of SynCAM1 strikingly depends on the presence of ST8SiaII[28], which is expressed at very low levels in the liver compared to ST8SiaIV, making it highly unlikely that SynCAM1 is the major polySia binding protein in the liver. We checked the immune-expression of neuropilin-2 and MARCKS in CDE and DDC damaged liver tissues and in BMOL cells. Only neuropilin-2 could be detected, and was restricted to endothelial cells of

damaged livers, suggesting that these 2 proteins are not binding protein in the liver. We therefore concluded that NCAM is the major binding protein of polySia in liver, a similar situation to that seen in the brain (Supplemental figure 10).

Here we propose a 3 step mechanism for NCAM and polySia in liver regeneration: 1) NCAM contributes to the cell-cell and cell-matrix interaction of HPCs in the un-activated HPC niche in normal liver. 2) During liver damage, polySia facilitates DR and HPC cell migration. 3) During the differentiation of HPCs to hepatocytes, NCAM is cleaved from the cell surface (Figure 8). We believe this 3 step NCAM, polySia-NCAM system modulates liver regeneration and importantly stops the further migration of cells once differentiated. Blockade of this “cellular lubrication system” can result in impaired DRs and liver regeneration. The therapeutic modulation of polySia levels and polySia-NCAM interactions may therefore be worth exploring in future studies.

REFERENCES

1. Bird TG, Lorenzini S, Forbes SJ. Activation of stem cells in hepatic diseases. Cell Tissue Res 2008;331:283-300.
2. Bird TG, Lu WY, Boulter L, Gordon-Keylock S, Ridgway RA, Williams MJ, et al. Bone marrow injection stimulates hepatic ductular reactions in the absence of injury via macrophage-mediated TWEAK signaling. Proc Natl Acad Sci U S A 2013;110:6542-7.
3. Sackett SD, Li Z, Hurtt R, Gao Y, Wells RG, Brondell K, et al. Foxl1 is a marker of bipotential hepatic progenitor cells in mice. Hepatology 2009;49:920-9.
4. Boulter L, Govaere O, Bird TG, Radulescu S, Ramachandran P, Pellicoro A, et al. Macrophage-derived Wnt opposes Notch signaling to specify hepatic progenitor cell fate in chronic liver disease. Nat Med 2012;18:572-9.
5. Lorenzini S, Bird TG, Boulter L, Bellamy C, Samuel K, Aucott R, et al. Characterisation of a stereotypical cellular and extracellular adult liver progenitor cell niche in rodents and diseased human liver. Gut 2010;59:645-54.
6. Hoffman S, Sorkin BC, White PC, Brackenbury R, Mailhammer R, Rutishauser U, et al. Chemical characterization of a neural cell adhesion molecule purified from embryonic brain membranes. J Biol Chem 1982;257:7720-9.
7. Acheson A, Sunshine JL, Rutishauser U. NCAM polysialic acid can regulate both cell-cell and cell-substrate interactions. J Cell Biol 1991;114:143-53.
8. Kleene R, Schachner M. Glycans and neural cell interactions. Nat Rev Neurosci 2004;5:195-208.
9. Hildebrandt H, Muhlenhoff M, Gerardy-Schahn R. Polysialylation of NCAM. Adv Exp Med Biol 2010;663:95-109.
10. Johnson CP, Fujimoto I, Rutishauser U, Leckband DE. Direct evidence that neural cell adhesion molecule (NCAM) polysialylation increases intermembrane repulsion and abrogates adhesion. J Biol Chem 2005;280:137-45.
11. Rutishauser U. Polysialic acid in the plasticity of the developing and adult vertebrate nervous system. Nat Rev Neurosci 2008;9:26-35.
12. Weinhold B, Seidenfaden R, Rockle I, Muhlenhoff M, Schertzinger F, Conzelmann S, et al. Genetic ablation of polysialic acid causes severe neurodevelopmental defects rescued by deletion of the neural cell adhesion molecule. J Biol Chem 2005;280:42971-7.
13. Hildebrandt H, Muhlenhoff M, Oltmann-Norden I, Rockle I, Burkhardt H, Weinhold B, et al. Imbalance of neural cell adhesion molecule and polysialyltransferase alleles causes defective brain connectivity. Brain 2009;132:2831-8.
14. Stummeyer K, Dickmanns A, Muhlenhoff M, Gerardy-Schahn R, Ficner R. Crystal structure of the polysialic acid-degrading endosialidase of bacteriophage K1F. Nat Struct Mol Biol 2005;12:90-6.
15. Hildebrandt H, Dityatev A. Polysialic Acid in Brain Development and Synaptic Plasticity. Top Curr Chem 2013.
16. Knittel T, Aurisch S, Neubauer K, Eichhorst S, Ramadori G. Cell-type-specific expression of neural cell adhesion molecule (N-CAM) in Ito cells of rat liver. Up-regulation during in vitro activation and in hepatic tissue repair. Am J Pathol 1996;149:449-62.
17. Nakatani K, Seki S, Kawada N, Kobayashi K, Kaneda K. Expression of neural cell adhesion molecule (N-CAM) in perisinusoidal stellate cells of the human liver. Cell Tissue Res 1996;283:159-65.
18. Nakatani K, Tanaka H, Ikeda K, Sakabe M, Kadoya H, Seki S, et al. Expression of NCAM in activated portal fibroblasts during regeneration of the rat liver after partial hepatectomy. Arch Histol Cytol 2006;69:61-72.
19. Fabris L, Strazzabosco M, Crosby HA, Ballardini G, Hubscher SG, Kelly DA, et al. Characterization and Isolation of Ductular Cells Coexpressing Neural Cell Adhesion Molecule and Bcl-2 from Primary Cholangiopathies and Ductal Plate Malformations. The American Journal of Pathology 2000;156:1599-1612.
20. Sonzogni A, Colloredo G, Fabris L, Cadamuro M, Paris B, Roffi L, et al. Isolated idiopathic bile ductular hyperplasia in patients with persistently abnormal liver function tests. J Hepatol

2004;40:592-8.
21. Zhou H, Rogler LE, Teperman L, Morgan G, Rogler CE. Identification of hepatocytic and bile ductular cell lineages and candidate stem cells in bipolar ductular reactions in cirrhotic human liver. Hepatology 2007;45:716-24.
22. Tsuchiya A, Kamimura H, Takamura M, Yamagiwa S, Matsuda Y, Sato Y, et al. Clinicopathological analysis of CD133 and NCAM human hepatic stem/progenitor cells in damaged livers and hepatocellular carcinomas. Hepatol Res 2009;39:1080-90.
23. Oltmann-Norden I, Galuska SP, Hildebrandt H, Geyer R, Gerardy-Schahn R, Geyer H, et al. Impact of the polysialyltransferases ST8SiaII and ST8SiaIV on polysialic acid synthesis during postnatal mouse brain development. J Biol Chem 2008;283:1463-71.
24. Tirnitz-Parker JE, Tonkin JN, Knight B, Olynyk JK, Yeoh GC. Isolation, culture and immortalisation of hepatic oval cells from adult mice fed a choline-deficient, ethionine-supplemented diet. Int J Biochem Cell Biol 2007;39:2226-39.
25. Tsuchiya A, Heike T, Fujino H, Shiota M, Umeda K, Yoshimoto M, et al. Long-term Extensive Expansion of Mouse Hepatic Stem/Progenitor Cells in a Novel Serum-Free Culture System. Gastroenterology 2005;128:2089-2104.
26. Espanol-Suner R, Carpentier R, Van Hul N, Legry V, Achouri Y, Cordi S, et al. Liver progenitor cells yield functional hepatocytes in response to chronic liver injury in mice. Gastroenterology 2012;143:1564-1575 e7.
27. Ono S, Hane M, Kitajima K, Sato C. Novel regulation of fibroblast growth factor 2 (FGF2)-mediated cell growth by polysialic acid. J Biol Chem 2012;287:3710-22.
28. Muhlenhoff M, Rollenhagen M, Werneburg S, Gerardy-Schahn R, Hildebrandt H. Polysialic Acid: Versatile Modification of NCAM, SynCAM 1 and Neuropilin-2. Neurochem Res 2013.
29. Galuska SP, Rollenhagen M, Kaup M, Eggers K, Oltmann-Norden I, Schiff M, et al. Synaptic cell adhesion molecule SynCAM 1 is a target for polysialylation in postnatal mouse brain. Proc Natl Acad Sci U S A 2010;107:10250-5.
30. Curreli S, Arany Z, Gerardy-Schahn R, Mann D, Stamatos NM. Polysialylated neuropilin-2 is expressed on the surface of human dendritic cells and modulates dendritic cell-T lymphocyte interactions. J Biol Chem 2007;282:30346-56.
31. Theis T, Mishra B, von der Ohe M, Loers G, Prondzynski M, Pless O, et al. Functional role of the interaction between polysialic acid and myristoylated alanine-rich C kinase substrate at the plasma membrane. J Biol Chem 2013;288:6726-42.

FIGURE LEGENDS

Figure 1. NCAM expression of normal and damaged livers in mouse by immunohistochemistry. The mRNA expression change of *Ncam*, *St8sia2* and *St8sia4*. (A-B) NCAM expression in normal mouse livers and CDE (A) and DDC (B) diet induced damaged livers. In normal mouse livers NCAM+ cells could be detected only on bile ducts or bile duct surrounding cells. After liver damage, NCAM+ DRs and their surrounding cells expanded aggressively from the portal tract in both liver damage models. (C-D) The mRNA change of *Ncam*, *St8sia2* and *St8sia4* before and after CDE and DDC diet induced liver damage. After liver damage, while the mRNA of *Ncam* and *St8sia4* increased significantly in both models, the mRNA levels of *St8sia2* did not change significantly. Scale bar = 100μm.

Figure 2. Characterization of NCAM+ cells and localisation of polySia+ cells in damaged livers by immunofluorescence staining. NCAM and polySia expression in human damaged livers. (A and B) Double immunofluorescence staining between NCAM and the ductular/HPC marker panCK (A) and sox9 (B) revealed that some cells of the bile duct and DR expressed NCAM (A and B; yellow arrows). Some cells surrounding the DR also expressed NCAM (A and B; green arrows). (C) Double immunofluorescence staining between NCAM and myofibroblast marker α-SMA revealed that some of the non-ductular NCAM+ cells were α-SMA+ myofibroblasts (C; yellow arrow. Green arrow shows α-SMA-/NCAM+ cells). (D) Immunofluorescence staining for polySia revealed that polySia was predominantly expressed at lateral cell surface of DRs (CK19+ cells were showed by serial section). (E) Immunohistochemistry using serial sections showed that chronic damaged human livers caused by hepatitis C virus (HCV), alcohol and primary biliary cirrhosis (PBC) also expressed NCAM and polySia on CK19+ DRs. Scale bar = 100μm (A and C) and 50μm (B, D and E).

Figure 3. Analysis of the role of polySia *in vitro*. (A) Double immunofluorescence staining for NCAM and polySia revealed that BMOL cells were positive for NCAM and polySia. Flow cytometric analysis showed that almost all cells are positive for NCAM some of which were positive for polySia with

different levels. Western blot analysis for NCAM without endoN revealed that anti-NCAM antibody detected diffuse signal, corresponding to polySia with NCAM, on lanes of P1.5 wild type mouse brain and BMOLs. After cleavage of polySia by endoN the bands were concentrated at 180kDa and 140kDa in P1.5 wild type mouse brain lane, and at 140 kDa in BMOLs lane. In lanes of NCAM knock out mouse brain no band could be detected. (B) Adhesion assay. After addition of endoN the number of adherent cells to laminin increased. (C) Cleavage of polySia by endoN did not affect cell expansion, even in the presence of HGF. (D) Aggregation assay. After the cleavage of polySia by endoN, the frequency of single cells/total cells decreased significantly indicating greater cell-cell aggregation. (E) Migration assay. Cleavage of polySia by endoN decreased HGF induced cell migration significantly compared with control (no endoN) (Dotted lines show the distal end of migrated cells). Scale bar = 100μm.

Figure 4. The fate of polySia-NCAM during differentiation of HPCs to hepatocytes *in vitro*. (A) Flow cytometric analysis using BMOLs cultured for 2 (A) and 4 days (B) in differentiation conditions (Wnt3A, HGF, OSM vs control) markedly decreased the frequency of polySia+ cells. Especially 4 days after addition of OSM strikingly decreased polySia. (C) While addition of Wnt3A and HGF decreased the mRNA of *St8sia4*, addition of OSM increased the mRNA of *Ncam* and *St8sia4* at day1 despite the frequency of polySia decreased at day2. (D) Western blot analysis of BMOL cell lysate with endoN after addition of OSM showed loss of NCAM protein. (E) In contrast, the western blot analysis of the BMOL culture media supernatant with endoN revealed that the addition of OSM increased the NCAM protein in the supernatant.

Figure 5. Characterization NCAM+ myofibroblasts and migration of the HPCs in the presence of NCAM+ myofibroblasts. (A) We characterised 2 cells lines NHNPC1 and NHNPC2 as myofibroblasts that expressed NCAM and α-SMA. (B) Both NHNPC1 and NHNPC2 expressed *α-SMA*, *Fibulin-2*, *Collagen-1* and *Desmin* but were negative for *Gfap* mRNA. (C) Flow cytometric analysis of NHNPCs

revealed that the frequency of polySia expression in NHNPCs was extremely low. (D) Schematic of the co-culture between NHNPC1 and BMOL. (E) Distance of migration (24 hours). Co-culture between NHNPC1 and BMOL with time lapse photography showed that BMOL migration was inhibited by 30% when polySia was cleaved with endoN (Supplemental videos 1 (control) and 2 (with endoN)). Scale bar = 100μm.

Figure 6. Analysis of the role of polySia during liver development. (A and B) HPC from E13.5 fetal HPCs expressed NCAM (A) and polySia (B). (C) H&E staining of wild type, *St8sia2*$^{+/-}$*4*$^{+/-}$ mice and *St8sia2*$^{-/-}$*4*$^{-/-}$ mice revealed grossly abnormal portal tracts in the knockout mice and normal portal tracts in the wild type mice. Immunohistochemistry for panCK revealed that the number of tube forming bile duct (bile ducts with typical morphology; black arrows) was less in *St8sia2*$^{+/-}$*4*$^{+/-}$ and *St8sia2*$^{-/-}$*4*$^{-/-}$ mice. (D) The frequency of tube forming bile ducts/portal area revealed a significant decrease in the number of tube forming bile duct in *St8sia2*$^{+/-}$*4*$^{+/-}$ and *St8sia2*$^{-/-}$*4*$^{-/-}$ mice compared to wild type mice. (E) Up-regulation of many biliary and HPC marker genes (*Ck19, Ggt, Sox9, Prominin-1,* and *Ncam*) could be detected in *St8sia2*$^{-/-}$*4*$^{-/-}$ mice compared to wild type mice. Scale bar = 100μm

Figure 7. Analysis of the role of polySia during DDC induced liver damage. (A) PanCK (DAB) staining revealed DRs/HPCs migrating into the parenchyma (black arrows) were more obvious in control group compared to endoN treated mice. (B) In endoN treated mice, DRs/HPCs migrating into parenchyma/portal area decreased significantly. (C) Anaysis of LW/BW ratio revealed a significant decrease of LW/BW ratio in endoN injected animals. (D) Serum blood test revealed only the serum ALT levels in endoN injection group were significantly elevated. (E) Real-time PCR analysis revealed that the mRNA levels of *Ck19*, *Alb*, *Tat*, *Cps1* and *Collagen-1* were significantly increased in endoN injection group. Scale bar = 100μm

Figure 8. Overview of the role of NCAM and polySia-NCAM in the niche. 1) In niche NCAM-NCAM

homophilic cell adhesion and NCAM-matrix heterophilic interaction contribute the stable settlement of HPCs. 2) During migration in the HPC niche, polySia is produced mainly via ST8SiaIV from HPCs. PolySia weakens the cell-cell and cell-matrix interactions. In this context HPCs can move more easily. With polySia HGF is able to accelerate the migration of HPCs during regeneration. 3) During differentiation into hepatocytes, HGF and Wnt stimulation regulate polySia at the transcriptional level and OSM contributes to the cleavage of NCAM and polySia-NCAM from the cell surface. Therefore hepatocytes do not express NCAM.

Figure 1

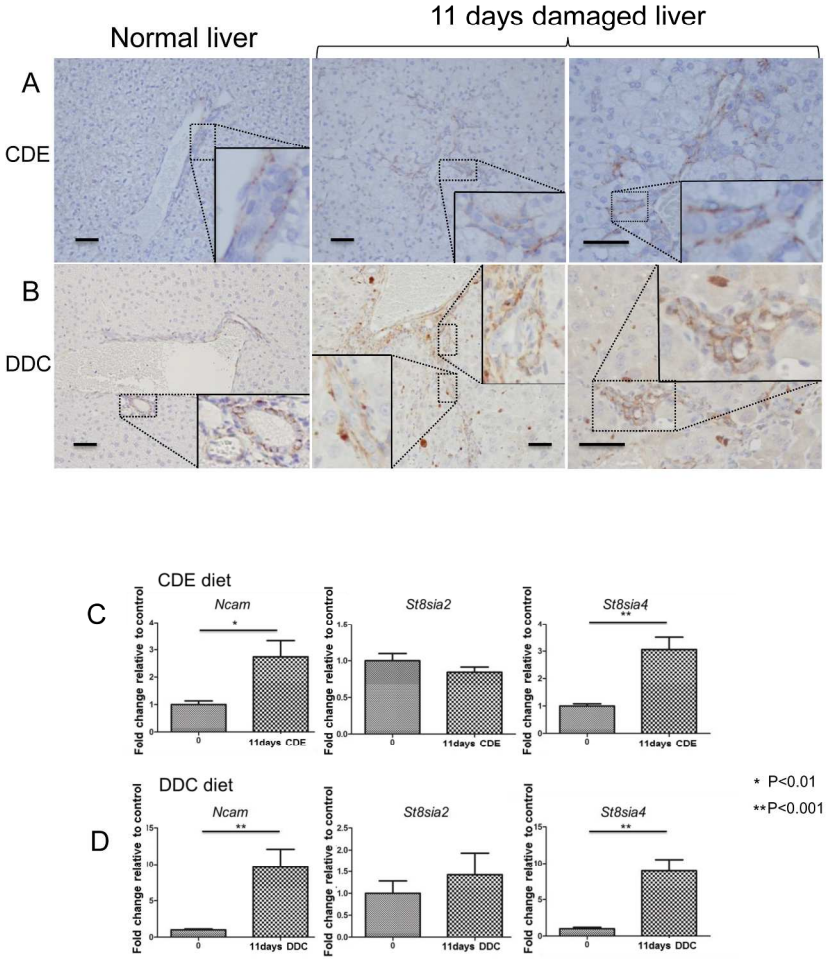

190x275mm (300 x 300 DPI)

Figure 2

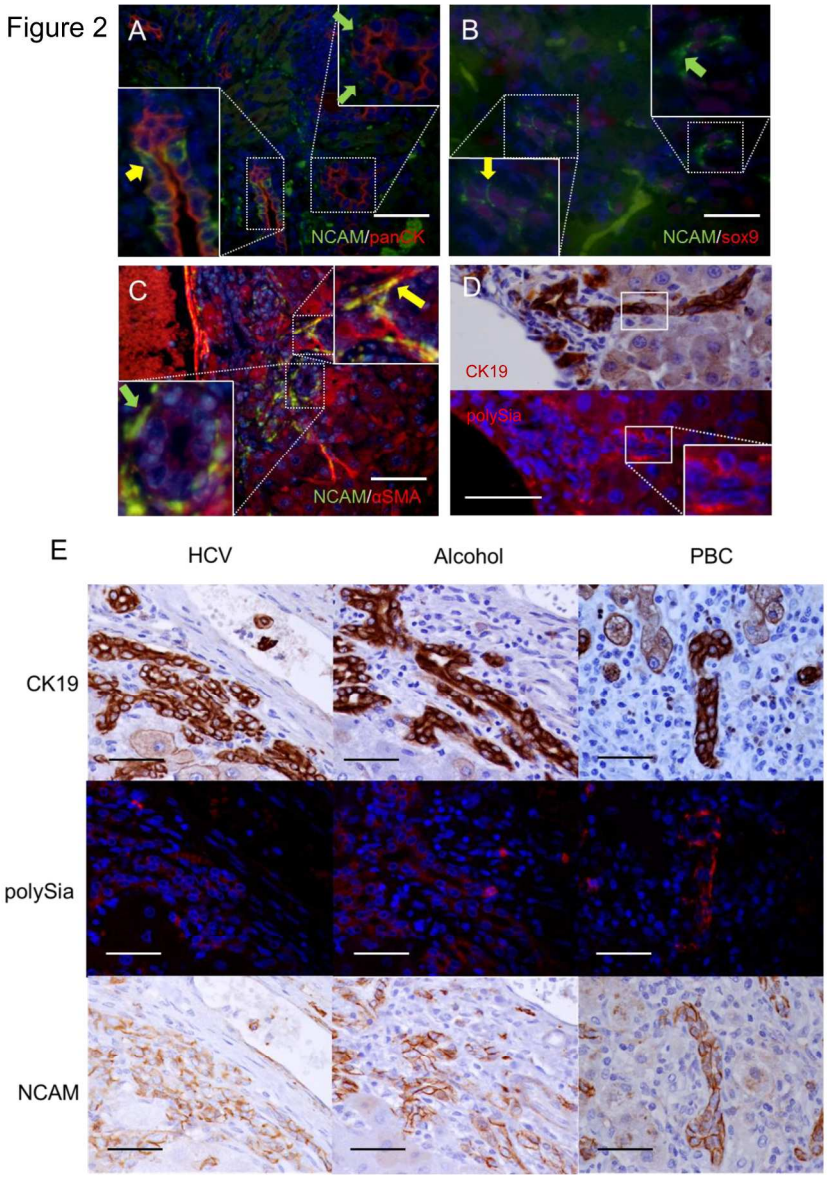

190x275mm (300 x 300 DPI)

Figure 3

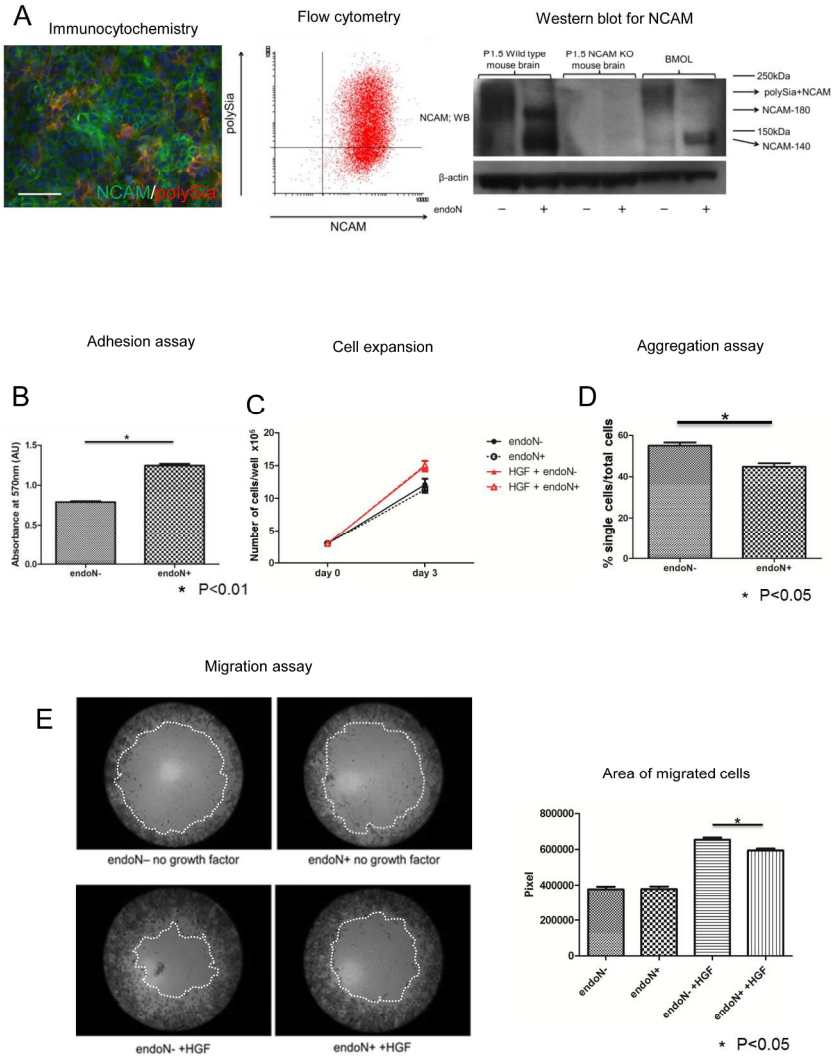

190x275mm (300 x 300 DPI)

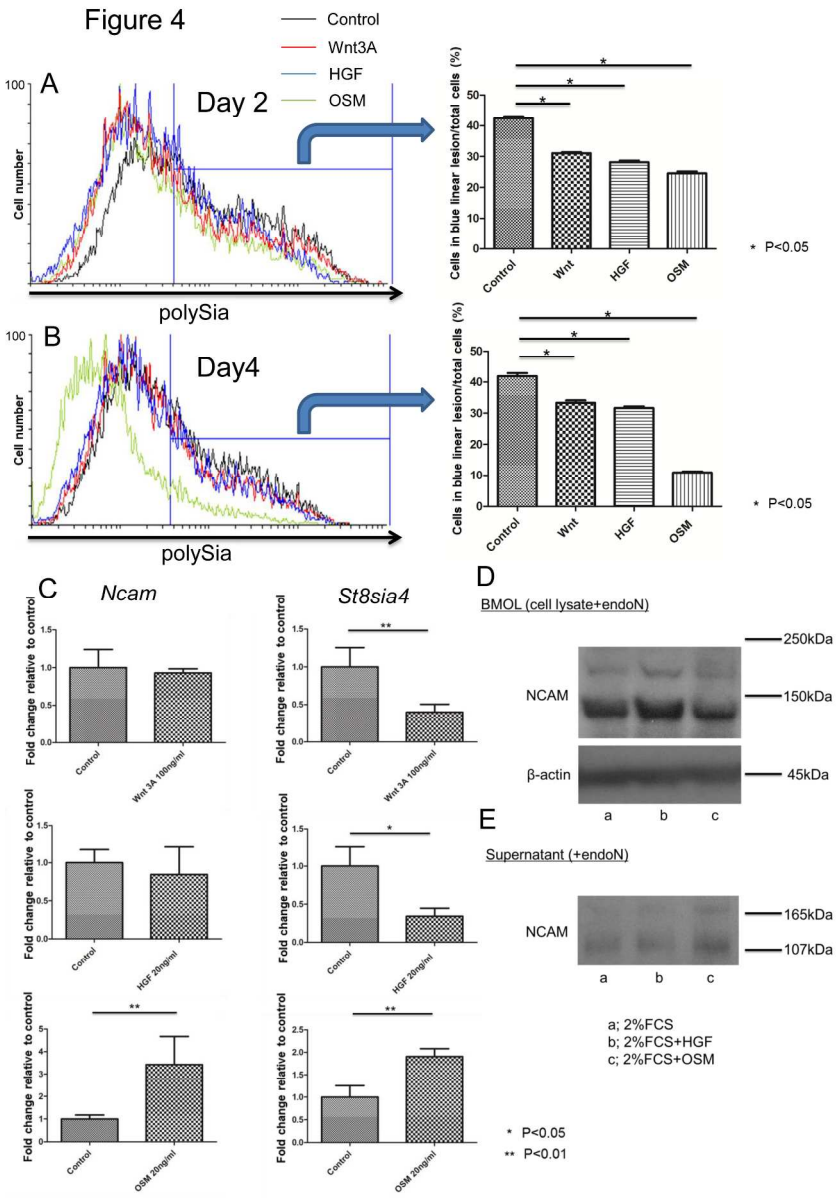

190x275mm (300 x 300 DPI)

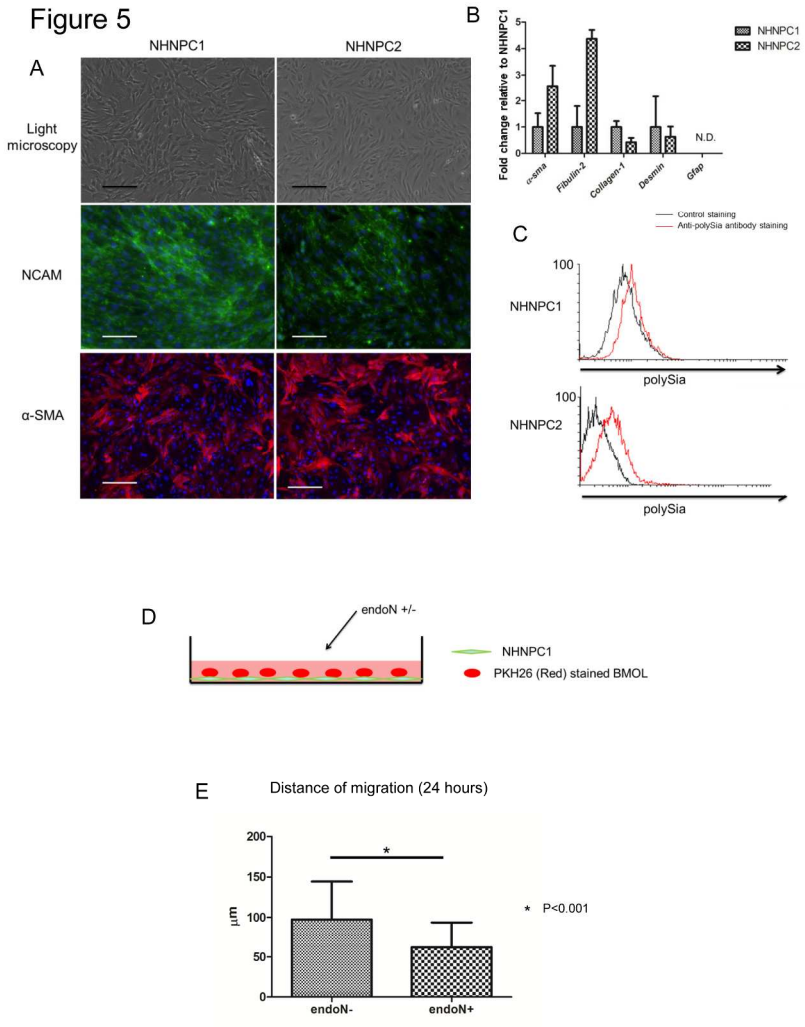

190x275mm (300 x 300 DPI)

Figure 6

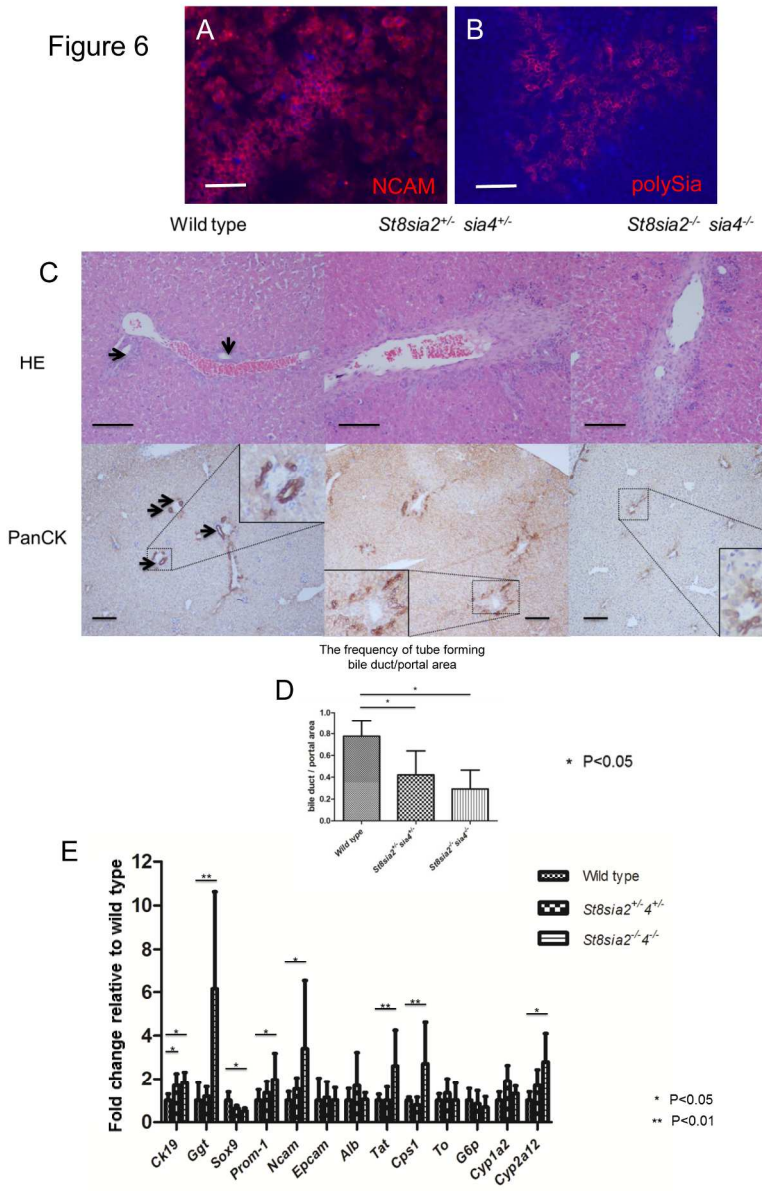

190x275mm (300 x 300 DPI)

Figure 7

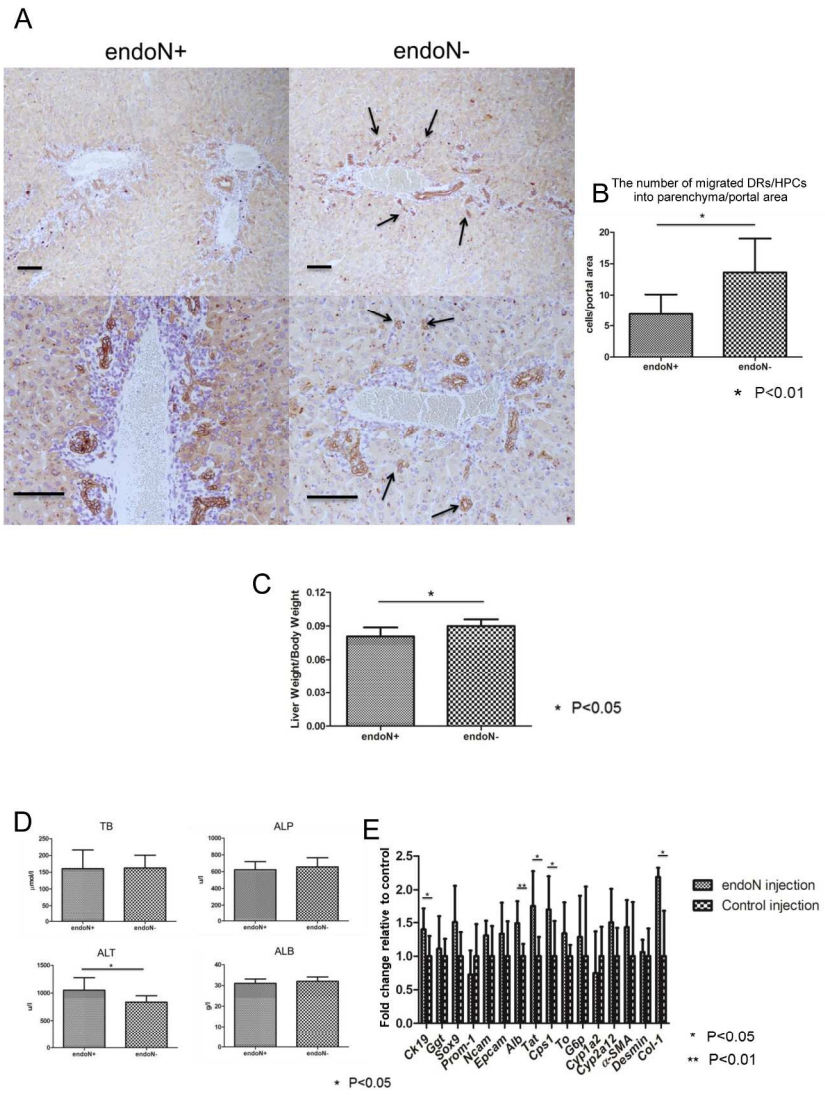

190x275mm (300 x 300 DPI)

Figure 8

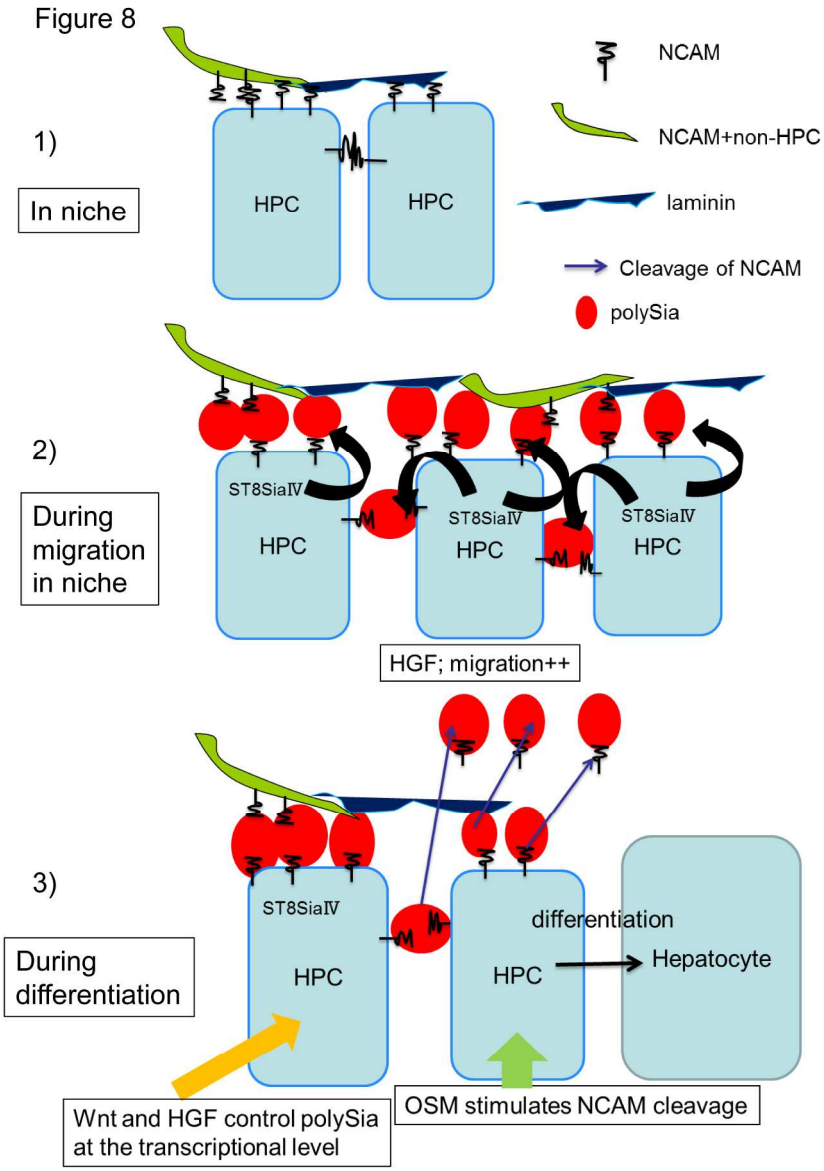

190x275mm (300 x 300 DPI)

SUPPLEMENTAL MATERIALS AND METHODS

Human liver tissue

We used archival cases of a chronic damaged liver caused by primary biliary cirrhosis (PBC), which was extirpated recipient livers from transplantation, and chronic damaged livers caused by hepatitis C and alcohol, which were resected for diagnosed HCC. Resected livers were analysed after their pathological diagnosis and receiving Institutional Review Board (IRB) approval from Niigata University.

Immunostaining

For immunohistochemistry, 10% formalin fixed tissue was cut to 5 μm were used. Where necessary, sections were antigen retrieved using heat mediated (10 mM sodium citrate buffer at PH6.0) or proteinase K enzymatic antigen retrieval. For DAB staining sections were blocked using 3% hydrogen peroxide for 10 minutes in room temperature (RT). Primary antibodies (Supplemental table 1) were incubated overnight at 4℃. Following this, species specific anti-IgG biotinylated antibodies were used for detection. Slides were then stained by Vectastain® ABC kit (Vector Laboratories, Inc. Burlingame, CA) and DAB substrate (DAKO, Glostroup, Denmark). Nuclei were stained using Mayer's hematoxylin solution. For fluorescence immunohistochemistry, single staining for polySia and double staining for NCAM with panCK, sox9, α-SMA, desmin, GFAP, CD45 and laminin were performed. (Anti-panCK antibody can detect identical populations of bile ducts and DRs with anti-CK19 antibodies as shown in Supplemental figure1). For polySia single staining, the mouse on mouse MOM kit (Vector) was used as per the manufacturer's protocol without antigen retrieval and then incubated with anti-polySia antibody followed by anti-mouse IgG Alexa555 conjugated antibody. For double fluorescence immunohistochemistry, NCAM antibodies were incubated overnight at 4℃. Sections were incubated with HRP conjugated anti-rabbit or rat IgG and detected by TSA™-plus Fluorescein System (PerkinElmer® Inc. Waltham, MA). Following this, tissues were stained as normal. Nuclei were labelled with DAPI mounting medium (SouthernBiotech, Birmingham, AL). For immunocytochemistry, cells

were washed with PBS, fixed with methanol at -20℃ for 10 minutes, and incubated with primary antibodies overnight at 4℃, and appropriate secondary antibodies for 30 minutes at RT. Nuclei were labelled with DAPI mounting medium. Photographs were taken using a Nikon Eclipse e600 microscope and camera (DXM1200F) and acquired using NIS-Elements D software (Nikon, Tokyo, Japan).

Histological analysis

To determine whether there was a difference between wild type, *St8sia2*$^{+/-}$*4*$^{+/-}$ and *St8sia2*$^{-/-}$*4*$^{-/-}$ mice, tube forming bile ducts (bile ducts with typical morphology)/portal area were analysed (3-10 portal areas/section were counted; wild type mice = 6, *St8sia2*$^{+/-}$*4*$^{+/-}$ mice = 7, *St8sia2*$^{-/-}$*4*$^{-/-}$ mice = 12). To analyse the difference of migrated cells in the DDC diet endoN injection study, panCK+ cells migrating into the liver parenchyma/portal area were counted (5-10 portal areas/section were counted, control mice = 9, endoN injected mice = 10). To confirm the NCAM and polySia expression in long term damaged mouse livers, 8 weeks DDC damaged liver tissues were stained using anti-NCAM, anti-CK19 and anti-polySia antibodies. To confirm the NCAM and polySia expression in human chronic liver diseases cirrhotic liver tissues caused by HCV, alcohol and PBC were stained using anti-NCAM, anti-CK19 and anti-polySia antibodies.

Western blot and co-immunoprecipitation

Liver cells and tissues from mice collected by M-per® Mammalian Protein Extraction Reagent (Thermo Scientific, Rockfold, IL) and culture media supernatant were clarified by centrifugation. Positive control (P1.5 wild type neonatal mouse brain tissue lysate) and negative control (P1.5 NCAM knock out neonatal mouse brain tissue lysate) were provided by Professor Rita Gerardy-Schahn, Hannover University. To detect polySia, samples were denatured at 60℃ for 10 minutes (heating at high temperature destroys polySia). Proteins (20μg total protein per lane) were separated by NuPAGE

4-12% Bis-Tris Gel (Life Technologies, Grand Island, NY) and were electroblotted onto nitrocellulose membranes. Immunoblotting was carried out using primary antibodies (Supplemental table 1). Bound antibodies were detected using HRP conjugated species specific IgG and developed by Immobilon™ Western chemiluminescent HRP substrate (MilliPore Corporation, Billerica, MA). β-actin was used as the loading control. Representative blots out of 3 or more independent experiments are shown. Co-immunoprecipitation was performed using Pierce® Crosslink Magnetic IP/Co-IP kit (Thermo Scientific) as manufacturer's protocol. To confirm if NCAM is the binding protein of polySia, following immunoprecipitation for NCAM immunoprecipitates were analysed by western blot using anti-NCAM and anti-polySia antibody. Western blot using anti-NCAM antibody was performed with or without endoN.

PCR

Total RNA was isolated using RNAeasy Mini kit (Qiagen, Chatsworth, CA) according to the manufacturer's protocol. RNA was reverse transcribed using QuantiTect reverse transcription kit (Qiagen). Gene expression analysis was achieved using pre-validated QuantiTech primers (Supplemental table 2) with Quantifast SYBR reagent (Qiagen). Real-time PCR was conducted using LightCycler 480 (Roche Applied Science, Mannheim, Germany). The results were obtained by at least 3 separate samples. *Ppia* was used as a housekeeping gene. Fold change in relative gene expression from control was calculated using the ΔΔCT method with pooled control samples as a compartor.

Cell Culture

The HPC cell line BMOL was kindly provided by Prof George Yeoh, University of Western Australia and maintained in WilliamsE medium containing 2% FCS (Life Technologies) on poly-l-lysine coated plates. For establishment of 2 HPC lines, after liver digestion of CDE diet liver, non-parenchymal cells

were collected as previously reported[1, 2]. These cells were expanded crudely (HPC line 2) or after sorting CD133+EPCAM+CD24+ cells using a FACS aria II cell sorter (Becton Dickinson, San Jose, CA) (HPC line 3) in medium for HPC culture[3]. After HPC colonies formed (based upon morphology) these cells were maintained in HPC maintenance medium[1] with 1% FCS supplemented with growth factors EGF (Peprotech, Rocky Hill, NJ, 20 ng/ml), bFGF (Miltenyi Biotec, Inc., Auburn, CA, 20 ng/ml) and HGF (Peprotech, 20 ng/ml). For establishment of NHNPC, after liver digestion of CDE diet liver, non-parenchymal cells were collected as previously reported[1, 2]. (We also tried to establish NHNPC using DDC diet damaged livers, however we could not establish.) These cells were expanded in medium for HPC culture[3] and after that growing fibroblastic colonies were picked up and maintained in 10% FCS containing WilliamsE medium with bFGF (20 ng/ml). All of these processes for establishment of HPC lines and NHNPCs were cultured using collagen-I coated plates. To harvest the BMOL cells for the following experiments diluted trypsin (500ml of PBS, 0.186g EDTA, 5ml of chicken serum (Sigma-Aldrich) and 5ml of 2.5% trypsin (Life Technologies) are mixed to make) that can keep polySia was used for 3 minutes. For the adhesion assay, cells were divided into two groups and cultured with endoN or without endoN overnight. $5x10^4$ BMOL cells were seeded in 96-well plates precoated with laminin (20 μg/ml) for 30 minutes. Cells were washed, and adherent cells were fixed in 5% glutaraldehyde (Sigma-Aldrich) and stained with 0.1% crystal violet. After dye solubilisation in 10% acetic acid, absorbance was measured at 570nm. For the expansion assay of BMOLs, 3×10^5 cells/well were cultured with or without endoN and counted 3 days later using cell counter chamber. HGF (20 ng/ml) were used for these experiments. To confirm whether NCAM protein expression in BMOLs was affected by HGF induced cell expansion, 3 days culture with or without HGF at 0, 20 and 50 ng/ml was performed and these cell lysates were examined by western blot for NCAM with endoN. For the aggregation assay, cells were cultured with or without endoN overnight. The cultured BMOLs were collected, washed 3 times and passed through a 27-gauge needle to make single cell suspension. Then, 2×10^5 cells/ml in 0.8% FCS contained PBS were incubated for 120 minutes in 15 ml conical tubes. During that time, cells were gently mixed every 30 minutes. We counted the viable

single cells and total cells using cell counter chamber and analysed the frequency of single cells/total cells. During counting dead cells were excluded by trypan blue. To assay migration, we used Oris™ Cell Migration Assay kit (Platypus Technologies, LLC. Madison, WI) as per the manufacturer's protocol. The area of migrating cells after 24 hours with or without endoN was calculated using Image J software. HGF (20 ng/ml) was used in this experiment. The results of all of these experiments were obtained from at least 4 separate experiments. For co-culture analysis, 6 x 10^5 NHNPC1 cells were seeded in 6 well collagen-I coated plates and cultured until they grew confluent. To stain BMOLs, PKH26 Red Fluorescent Cell linker for General Cell Membrane Labeling (Sigma-Aldrich) was used as per manufacturer's protocol. The PKH26 stained (red) 2 x 10^5 BMOLs were cultured on a NHNPC1 confluent cell monolayer with or without endoN. Pictures were taken every 20 minutes for 24 hours using Axio Obserber Z.1 (Carl Zeiss, Oberkochen, Germany) and distance of cell migration (randomly selected 60 cells of each group) was analysed. For differentiation of BMOLs towards hepatocytes, 3 x 10^5 cells/well were cultured without growth factors or with Wnt3A (100 ng/ml, Peprotech), HGF (20 ng/ml) or OSM (20 ng/ml, Sigma-Aldrich) for 1-4 days. For preparation of cell lysates and culture media supernatant for NCAM western blot, 6 x 10^5 cells/well were cultured for 24 hours with or without growth factors (20 ng/ml of HGF or 20 ng/ml of OSM). HPCs from E13.5 fetal livers used for immunocytochemistry for NCAM and polySia were established previously in our group[1].

Flow cytometry

Cells were harvested with diluted trypsin (500ml of PBS, 0.186g EDTA, 5ml of chicken serum (Sigma-Aldrich) and 5ml of 2.5% trypsin (Life Technologies) are mixed to make) for 3 minutes to keep polySia. The resulting cells were incubated with anti-mouse CD16/32 antibody (Becton Dickinson) for 15 minutes on ice to block non-specific binding. Cells were then incubated with antibodies (Supplemental table 1) for 30 minutes on ice. After washing, cells were analysed by FACSCaliber (Becton Dickinson). Results of flow cytometry were obtained by at least 3 separate samples and analysed using Flowing Software 2.3.3 (Cell Imaging Core, Turku Centre for Biotechnology, Finland).

EndoN

For *in vitro* studies, endoN that was purchased from Eurobio Laboratories (AbC0020, CourtBoeuf Cedex, France) was employed according to the manufacturer's protocol. For *in vivo* studies, endoN was kindly provided by Professor Rita Gerardy-Schahn (Hannover University). 10 µg/ml of endoN from Hannover University was added to the liver tissue lysate for lanes 2 and 4 of test series.

Statistics

Statistical analyses were performed using GraphPad Prism5 software (GraphPad Software, Inc., La Jolla, CA). Data are presented as mean±SD. The results were assessed using Mann-Whitney test. Differences were considered significant when the P-value was less than 0.05.

REFERENCES

1. Tsuchiya A, Heike T, Fujino H, Shiota M, Umeda K, Yoshimoto M, et al. Long-term Extensive Expansion of Mouse Hepatic Stem/Progenitor Cells in a Novel Serum-Free Culture System. Gastroenterology 2005;128:2089-2104.
2. Tsuchiya A, Heike T, Baba S, Fujino H, Umeda K, Matsuda Y, et al. Long-term culture of postnatal mouse hepatic stem/progenitor cells and their relative developmental hierarchy. Stem Cells 2007;25:895-902.
3. Okabe M, Tsukahara Y, Tanaka M, Suzuki K, Saito S, Kamiya Y, et al. Potential hepatic stem cells reside in EpCAM+ cells of normal and injured mouse liver. Development 2009;136:1951-60.

SUPPLEMENTAL FIGURE LEGENDS

Supplemental figure 1. Comparison of staining pattern between anti-panCK and anti-CK19 antibodies. Both antibodies detected the same bile ducts and DRs in DDC damaged livers. (A; serial section, B; immunofluorescence double immunohistochemistry.) Scale bar = 100μm (A and upper panels of B) and 50μm (lower panels of B).

Supplemental figure 2. Characterization of NCAM+ cells in damaged livers by immunofluorescence staining. (A and B) Double immunofluorescence staining between NCAM and the ductular/HPC marker panCK (A) and sox9 (B) revealed that some cells of the bile duct and DR (A; yellow arrow) expressed NCAM. However some of the bile duct or DR surrounding cells (A and B; green arrows) also expressed NCAM. (C) Double immunofluorescence staining between NCAM and myofibroblast marker desmin revealed that some of the non-ductular NCAM+ cells were desmin+ myofibroblast (C; yellow arrows. Green arrows show desmin-/NCAM+ cells). (D and E) Double immunofluorescence staining between NCAM and stellate cell marker GFAP (D) and hematopoietic cell marker CD45 (E) revealed that NCAM+ cells were GFAP- and CD45-. Double immunofluorescence staining between NCAM and laminin showed that most of NCAM+ cells were in direct contact with laminin. Long term (8 weeks) DDC damaged liver also express NCAM (G) and polySia (H) in the same manner with short term DDC damaged livers shown in figure 1B and 2D. Scale bar = 50μm (A-C, G and H) and 100μm (D-F).

Supplemental figure 3. NCAM and polySia expression of three HPC lines. (A and B) Both of HPC line 2 and HPC line 3 expressed NCAM (green) and polySia (red). (C) The frequency of polySia in BMOLs was higher than that of other 2 cell lines. Scale bar = 100μm.

Supplemental figure 4. Differentiation of BMOL to hepatocytes. (A-C) Following the differentiation of BMOLs to hepatocytes with Wnt3A (A) or OSM (C), the gene expression of *Ck19* decreased, and the hepatocyte markers *Alb* increased significantly. (B) HGF which also induces expansion and migration

of BMOL has relatively weak differentiation induction ability compared to Wnt3A and OSM.

Supplemental figure 5. Co-immunoprecipitation analysis. After immunoprecipitation of NCAM protein using anti-NCAM antibody, western blot for NCAM and polySia were performed using the immunoprecipitates. We could detect diffuse band around 200kDa which showed NCAM with polySia (arrow) when immunoprecipitates were blotted for NCAM and polySia. After the endo-N treatment the band was concentrated to 140kDa (arrowhead) when detected using anti-NCAM antibody.

Supplemental figure 6. Characterization of NCAM and polySia expressing HPC cell line. (A) PCR analysis using BMOLs revealed that BMOLs expressed NCAM and the main enzyme that contributed to the production of polySia was ST8SiaIV. (B) Western blot analysis with endoN after addition of different concentration of HGF (0ng/ml, 20ng/ml and 50ng/ml; 3 days culture) showed that expansion by HGF did not affect the expression of NCAM protein.

Supplemental figure 7. A schematic of results of mouse models with gene defects in the polyST. In wild type neonatal mouse liver many tube forming bile ducts (bile ducts with typical morphology) could be detected. The number of tube forming bile ducts decreased in both *St8sia2*$^{+/-}$*4*$^{+/-}$ and *St8sia2*$^{-/-}$*4*$^{-/-}$ mice, particularly in *St8sia2*$^{-/-}$*4*$^{-/-}$ mice.

Supplemental figure 8. A schematic to examine the effect of endoN *in vivo*. (A) A schematic of this study. EndoN or control was injected 4 times intraperitoneally into mice with DDC induced liver injury. (B) Test series of endoN injection resulted in the cleavage of polySia in the liver. Lanes 1 and 3 are liver tissue lysates from control injected mice. Lanes 2 and 4 are tissue lysates treated with endoN to lanes 1 and 3 respectively after protein extraction to confirm the activity of endoN as positive controls. Lanes 5-10 are endoN injected tissue lysates at different doses. In all endoN injected groups polySia was cleaved from the livers compared to control treated animals.

Supplemental figure 9. A schematic of endoN injection study using DDC diet liver damage mouse models. In control mice (without endoN injection) many DR cells migrated into the parenchyma. In contrast PolySia cleavage by intraperitoneal endoN injection resulted in a reduction in the number of DR cells migrating into liver parenchyma.

Supplemental figure 10. Analysis of other possible polySia binding proteins in the liver by immunostaining. (A-F) Both MARCKS and neuropilin-2 could not be detected in bile ducts or DRs in CDE and DDC diet damaged livers and BMOL HPC line. Endothelial cells in CDE and DDC diet damaged livers are positive for neuropilin-2. Scale bar = 50μm (A-D) and 100μm (E and F).

Table 1. Primary antibodies used in this study.

Primary antibody	Species	Source	Dilution
Mouse NCAM	Rabbit	ProteinTech	IHC, ICC, 1/50; WB, 1/1000
Mouse NCAM (H28)	Rat	Gifted (Hannover Univ)	IHC, ICC, 1/100; WB1/1000
polySia (735)	Mouse	Gifted (Hannover Univ)	IHC, 1/500
polySia	Mouse	Miltenyi Biotec	ICC, 1/10; FACS, 1/30
cytokeratin19	Rat	Developmental Studies Hybridoma Bank	1/200
PanCK	Rabbit	DAKO	1/200
Sox 9	Rabbit	MILLIPORE	1/100
α-SMA	Mouse	Sigma-Aldrich	1/500
Desmin	Rabbit	Abcam	1/50
GFAP	Rabbit	Abcam	1/500
CD45	Rat	R&D systems	1/100
Laminin	Rabbit	Abcam	IHC, 1/25
MARCKS	Rabbit	Abcam	IHC,ICC, 1/100
Neuropilin-2	Rabbit	Cell Signaling	IHC,ICC, 1/100
β-actin	Rabbit	Sigma-Aldrich	1/5000

IHC, immunohistochemistry; ICC, immunocytochemistry; WB, western blot; FACS, flow cytometry

Table 2. PCR primers used in this study.

Name	Identification number
Ncam	QT01065064
St8sia2	QT00099750
St8sia4	QT00165522
Ck19	QT00156667
Ggt	QT00104209
Alb	QT00115570
Prominin-1	QT01065162
Sox 9	QT00163765
Epcam	QT02304456
Tat	QT00112833
Cps1	QT01049041
To	QT00150409
G6p	QT00114625
Cyp1a2	QT00100674
Cyp2a12	QT00115619
α-sma	QT00140119
Fibulin-2	QT00145943
Collagen 1a2	QT02325736
Desmin	QT00102333
Gfap	QT00101143
Ppia	QT00247709

Supplemental figure 1

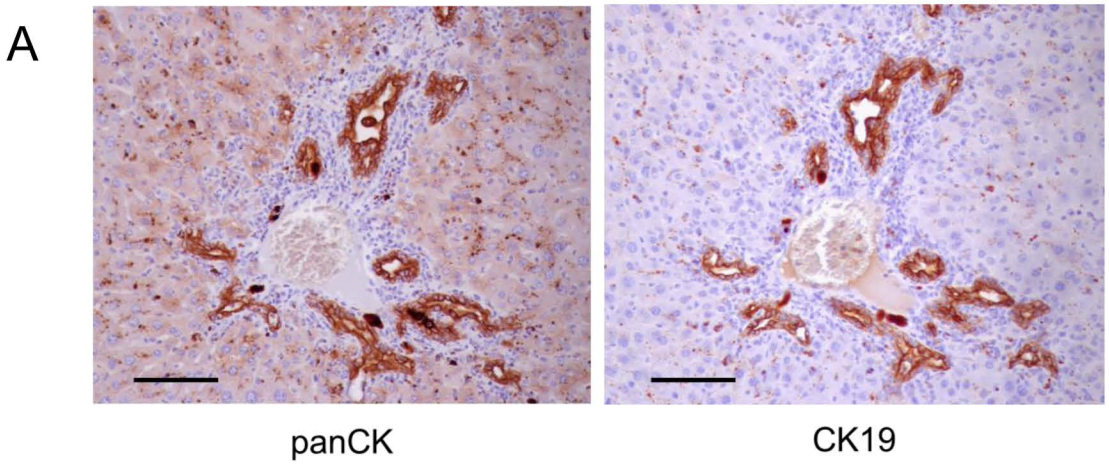

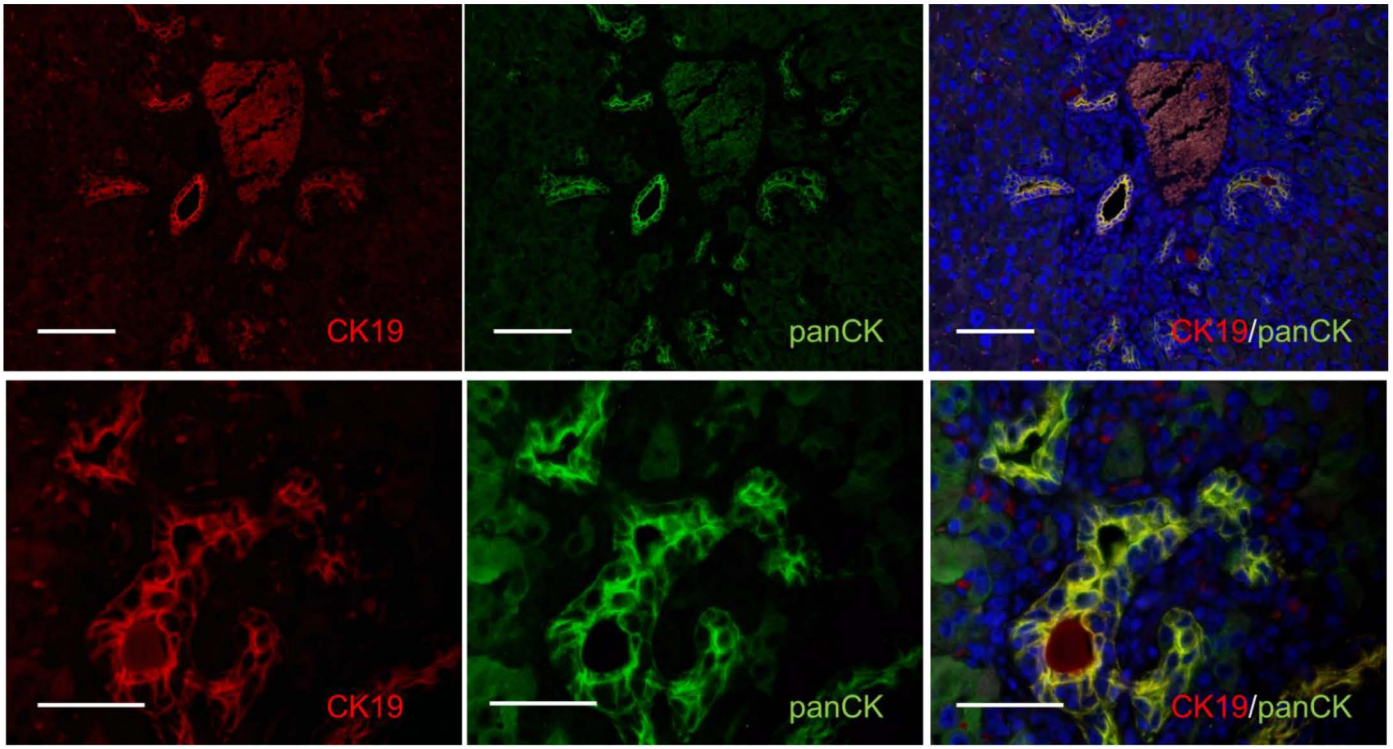

Supplemental figure 2

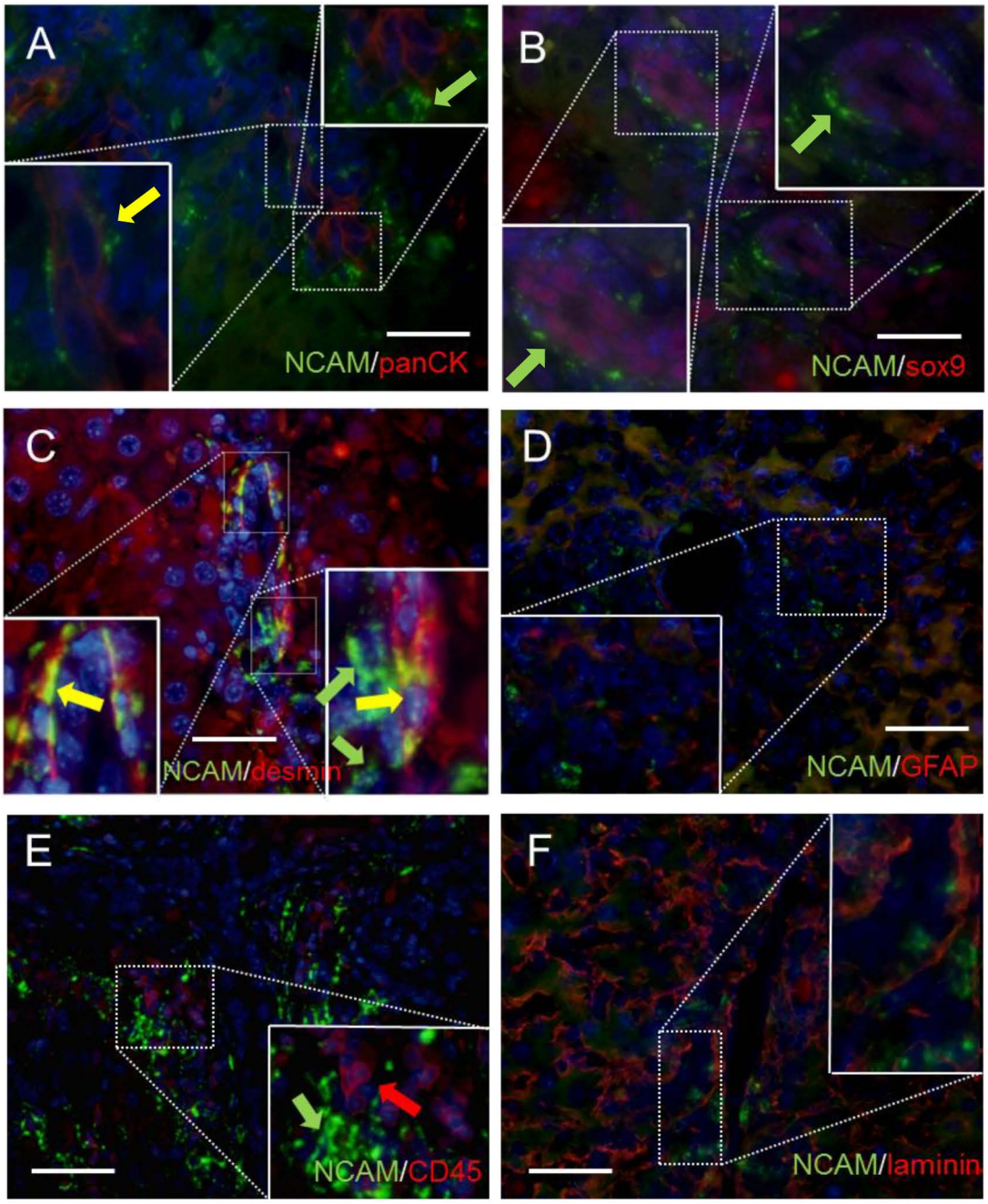

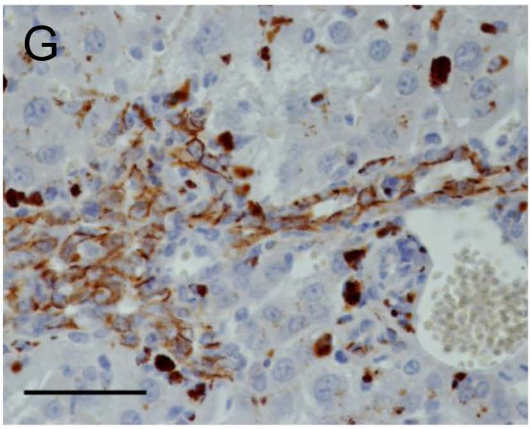

NCAM

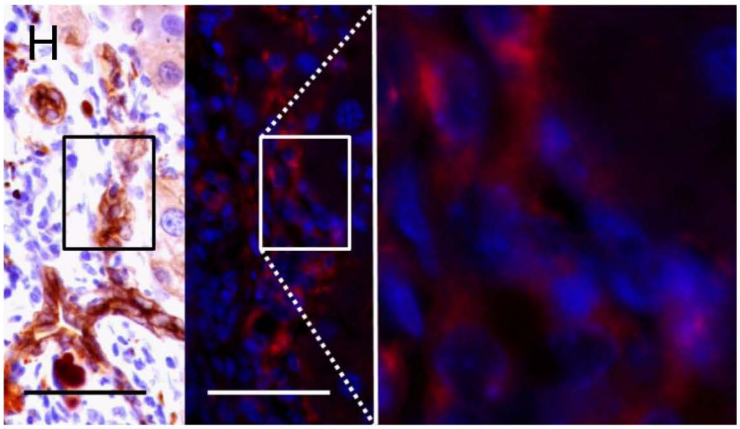

CK19 polySia

Supplemental figure 3

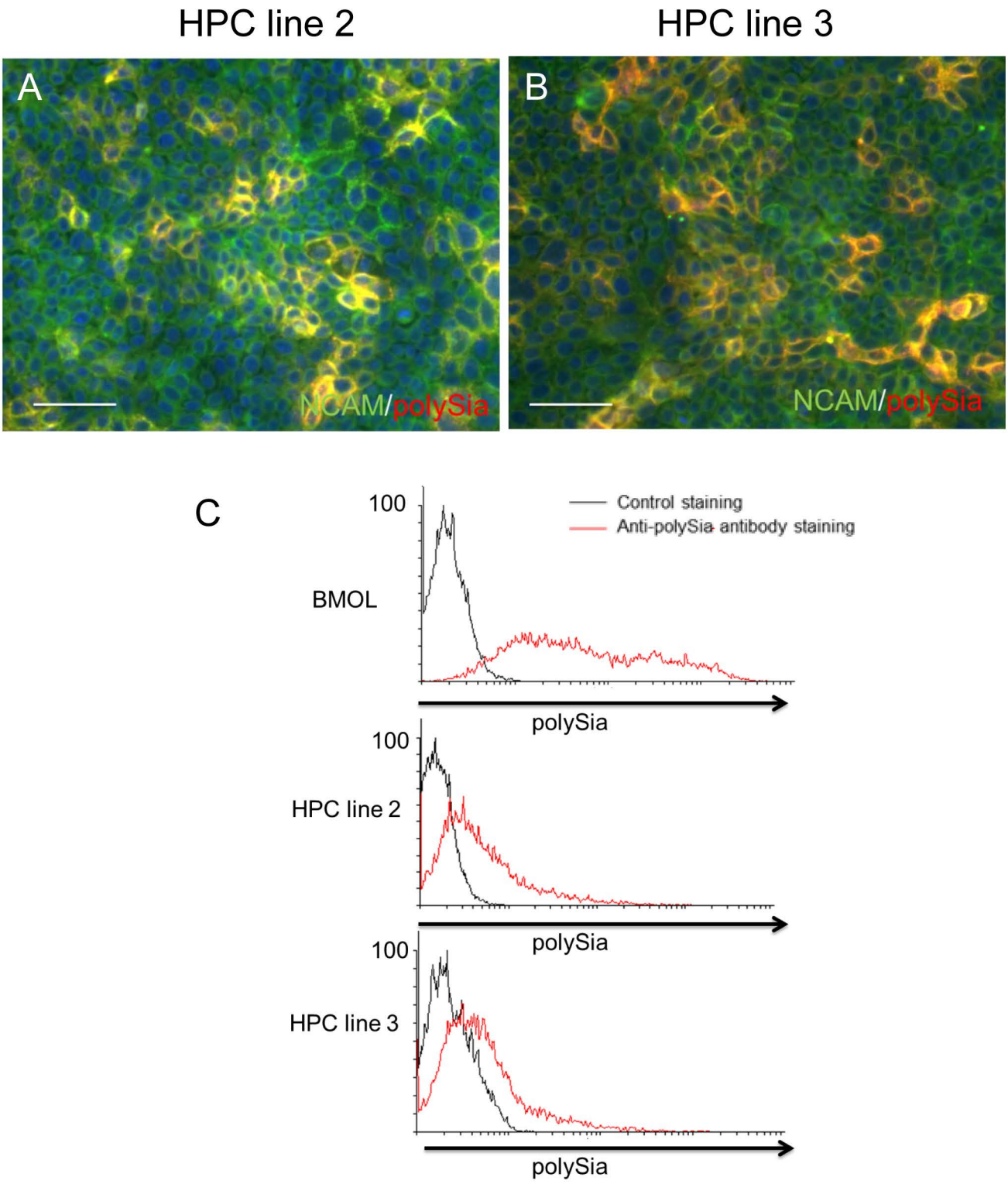

Supplemental figure 4

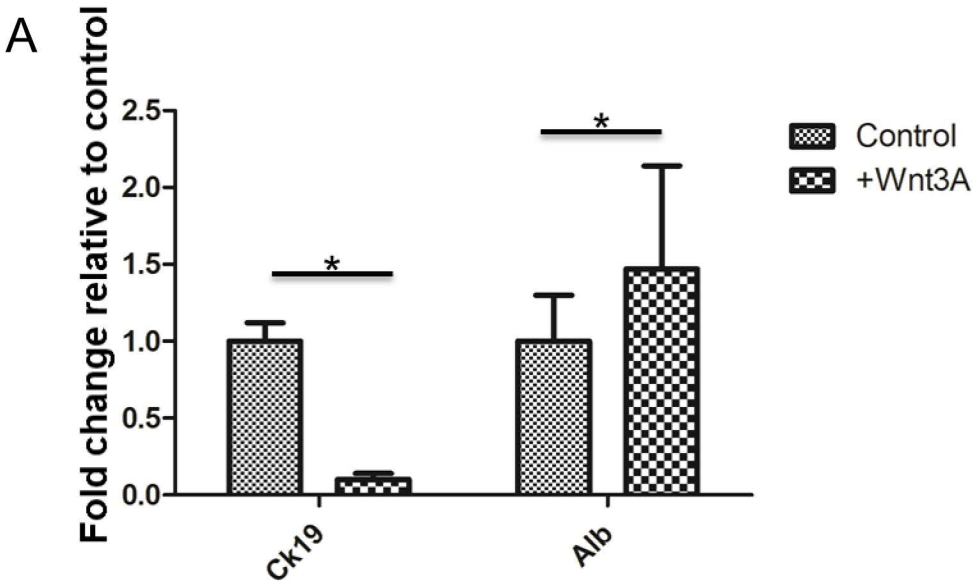

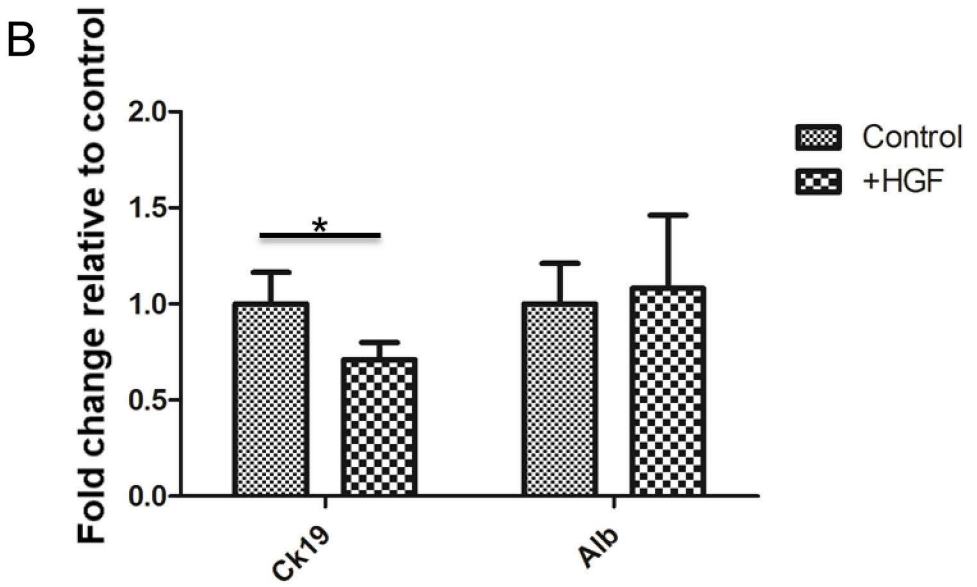

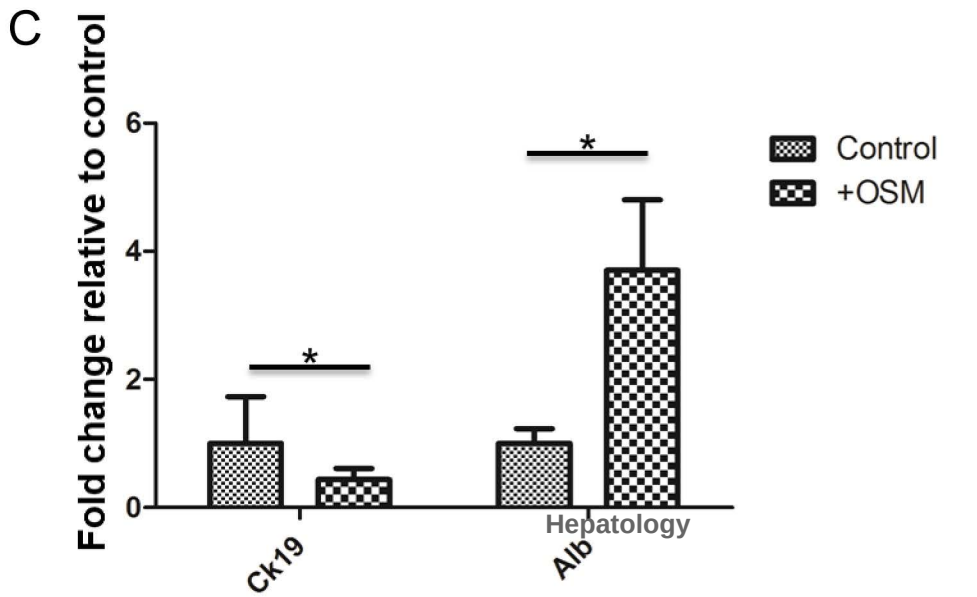

* P<0.05

Supplemental figure 5

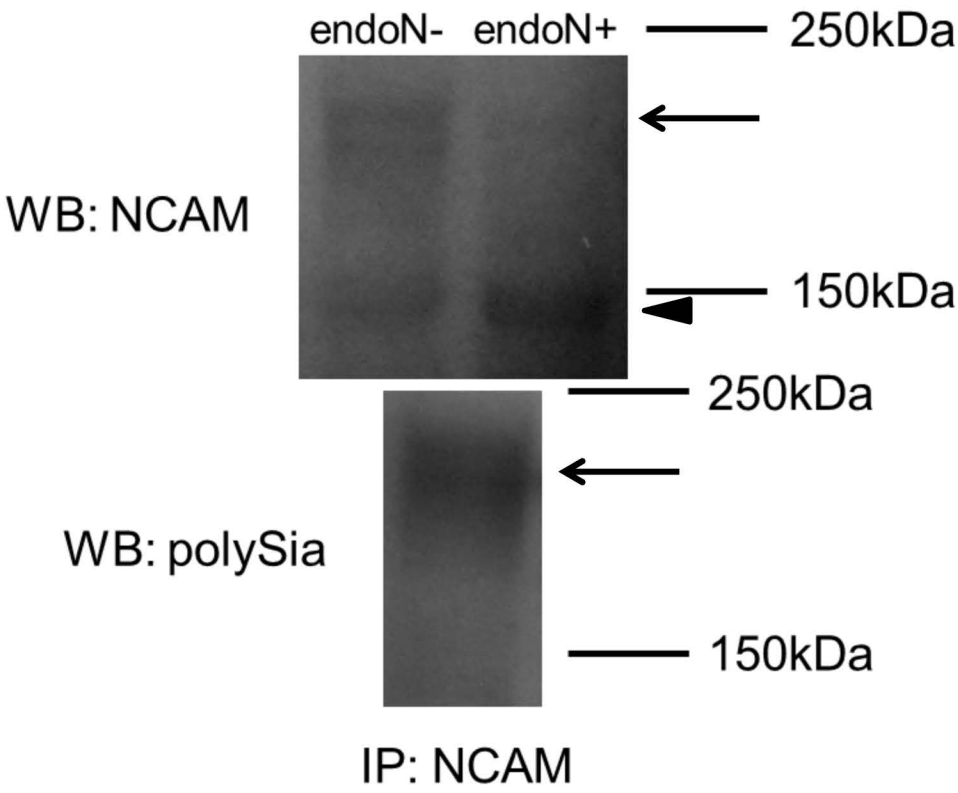

Supplemental figure 6

A

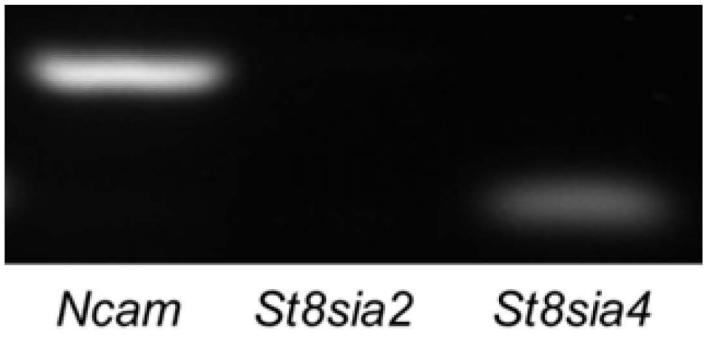

B

Western blot for NCAM after endoN treatment (cell lysate+endoN)

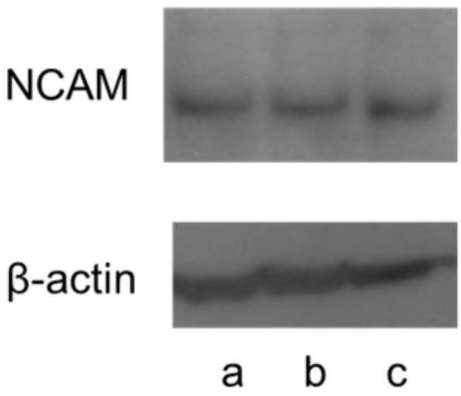

a; 2% FCS
b; 2% FCS+20ng/ml HGF
c; 2% FCS+50ng/ml HGF

Supplemental figure 7

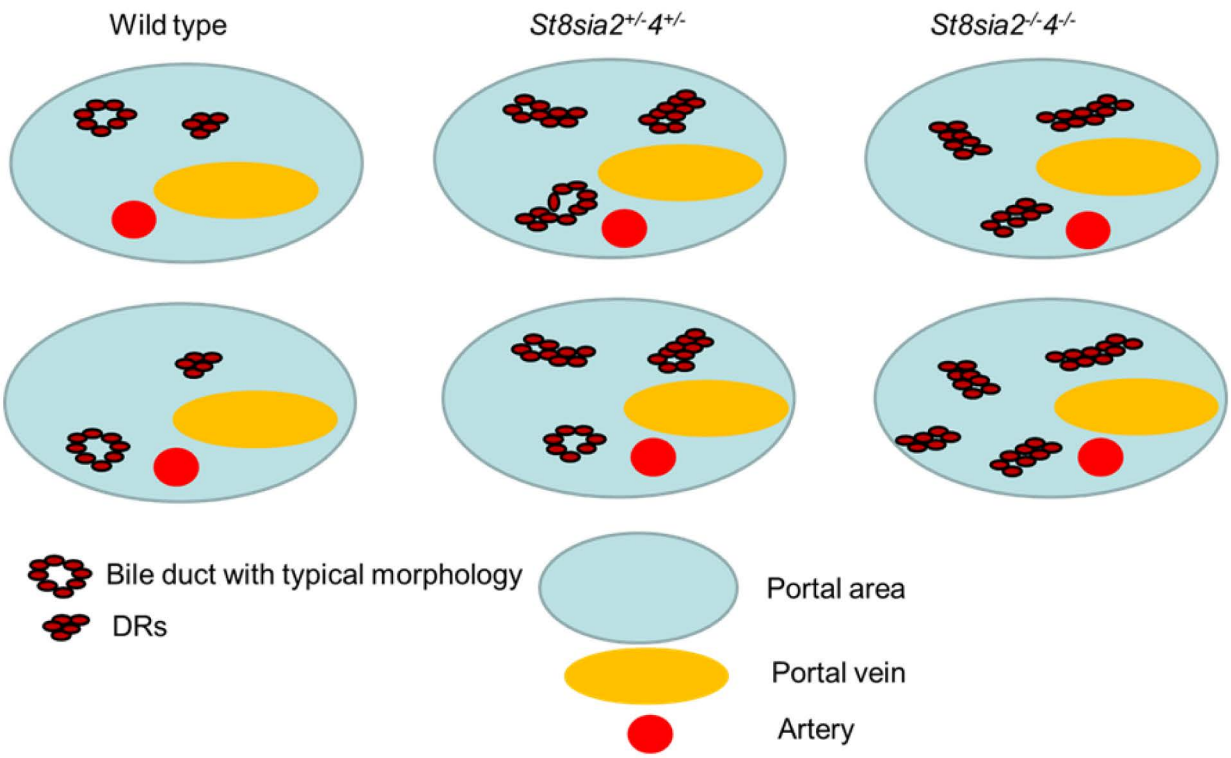

Supplemental figure 8

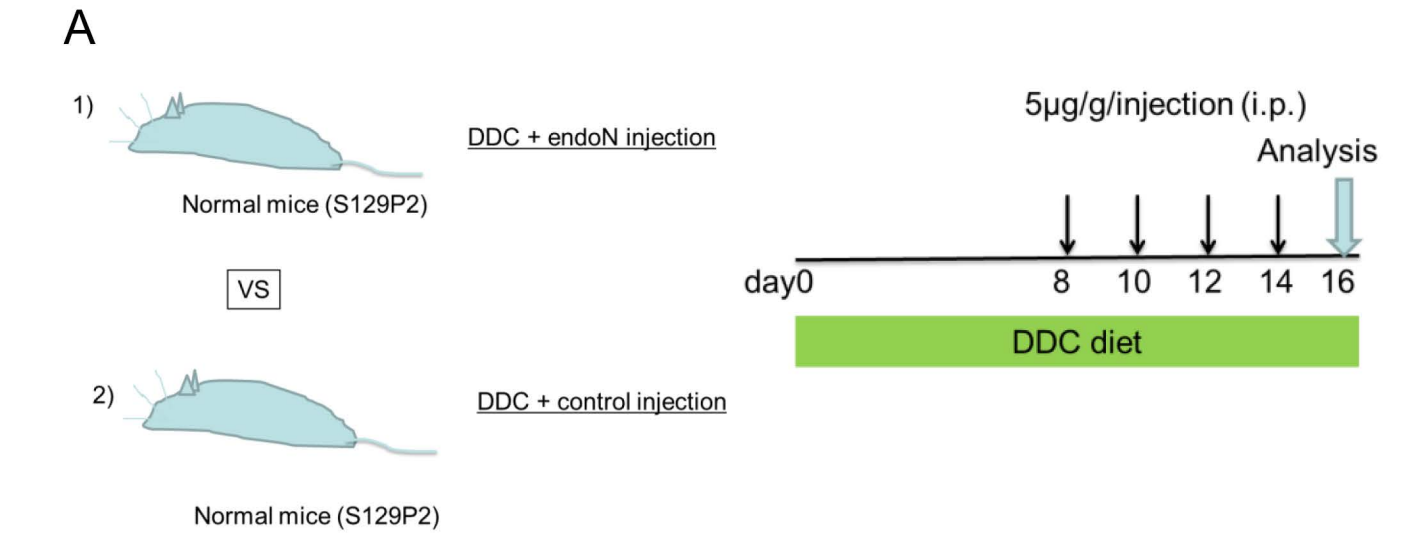

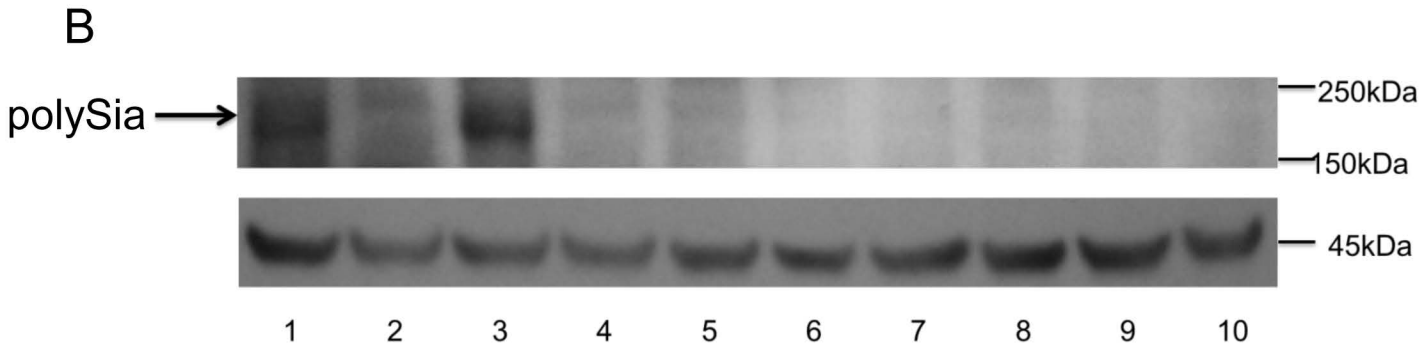

1. control 1
2. control 1 + endoN in tissue lysate
3. control 2
4. control 2 + endoN in tissue lysate
5. 3.14 μg/g of endoN injection
6. 3.51 μg/g of endoN injection
7. 7.58 μg/g of endoN injection
8. 8.65 μg/g of endoN injection
9. 17.61 μg/g of endoN injection
10. 19.69 μg/g of endoN injection

Supplemental figure 9

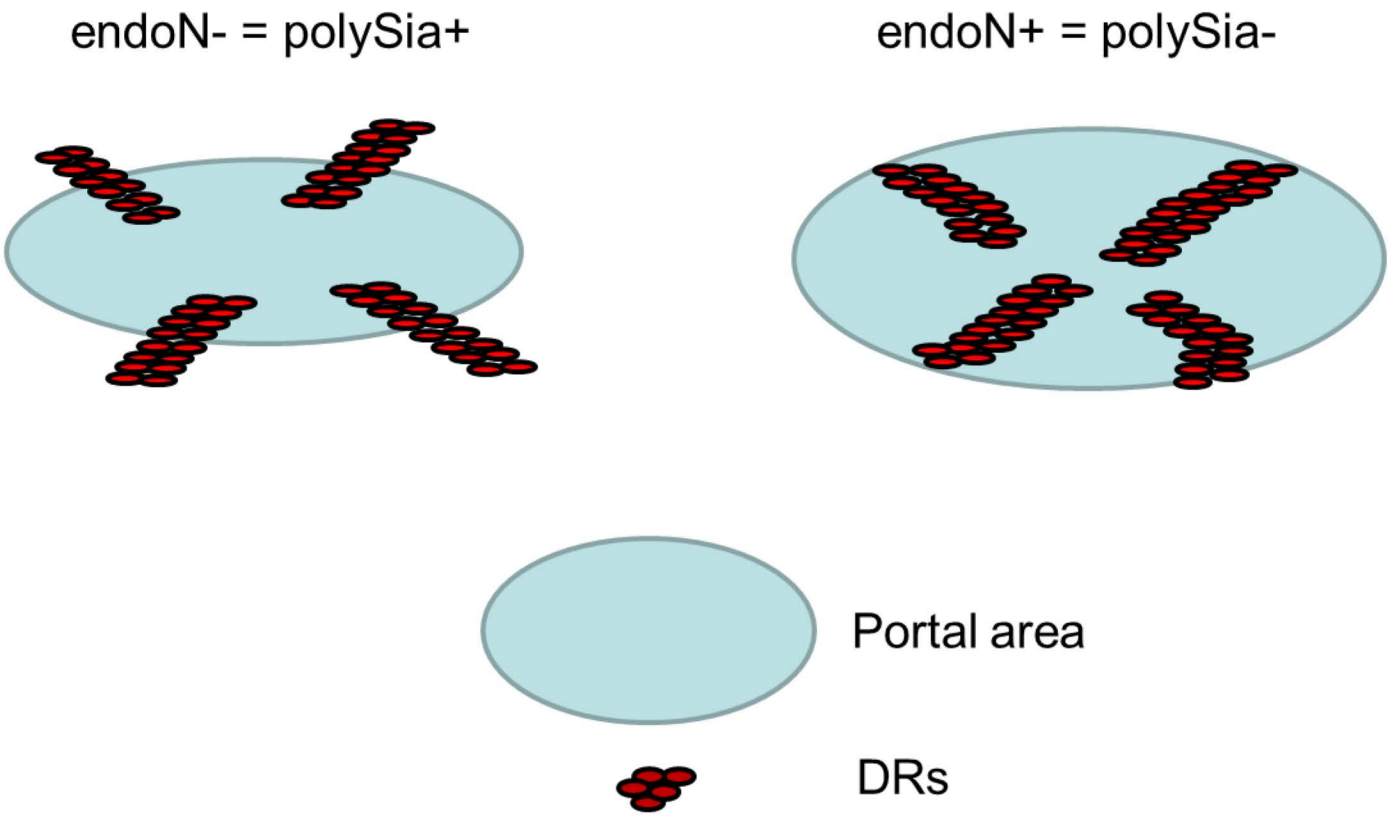

Supplemental figure 10